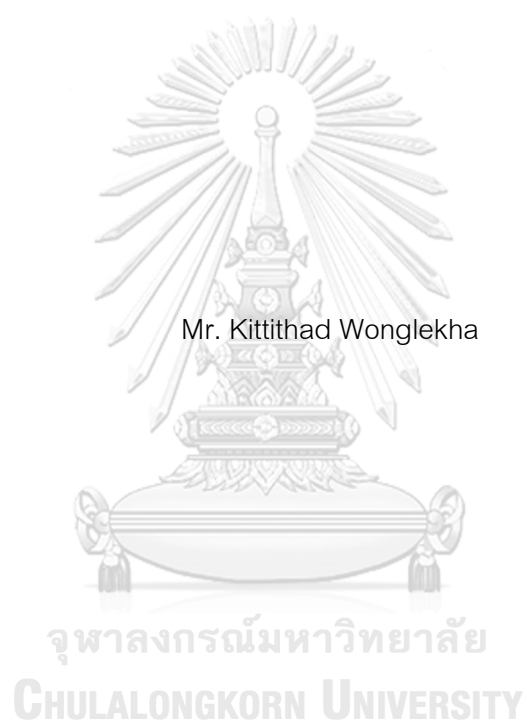


EFFECTS OF TiO_2 SUPPORT AND Co ADDITION ON Ni/TiO_2 CATALYSTS IN SELECTIVE
HYDROGENATION OF FURFURAL TO FURFURYL ALCOHOL



A Thesis Submitted in Partial Fulfillment of the Requirements
for the Degree of Master of Engineering in Chemical Engineering

Department of Chemical Engineering

Faculty of Engineering

Chulalongkorn University

Academic Year 2018

Copyright of Chulalongkorn University

ผลของตัวรองรับไทเทเนียมและการเติมโคบอลต์ต่อตัวเร่งปฏิกิริยา Ni/TiO₂ ในปฏิกิริยาไฮโดรจีเนชัน
แบบเลือกเกิดของเฟอร์ฟูรัลเป็นเฟอร์ฟิวรีดแอลกอฮอล์



วิทยานิพนธ์นี้เป็นส่วนหนึ่งของการศึกษาตามหลักสูตรปริญญาวิศวกรรมศาสตรมหาบัณฑิต
สาขาวิชาวิศวกรรมเคมี ภาควิชาวิศวกรรมเคมี
คณะวิศวกรรมศาสตร์ จุฬาลงกรณ์มหาวิทยาลัย
ปีการศึกษา 2561
ลิขสิทธิ์ของจุฬาลงกรณ์มหาวิทยาลัย

| | |
|----------------|---|
| Thesis Title | EFFECTS OF TiO ₂ SUPPORT AND Co ADDITION ON Ni/TiO ₂ CATALYSTS IN SELECTIVE HYDROGENATION OF FURFURAL TO FURFURYL ALCOHOL |
| By | Mr. Kittithad Wonglekha |
| Field of Study | Chemical Engineering |
| Thesis Advisor | Professor JOONGJAI PANPRANOT, Ph.D. |

Accepted by the Faculty of Engineering, Chulalongkorn University in Partial Fulfillment of the Requirement for the Master of Engineering

..... Dean of the Faculty of Engineering
(Professor SUPOT TEACHAVORASINSKUN, D.Eng.)

THESIS COMMITTEE

..... Chairman
(Associate Professor ANONGNAT SOMWANGTHANAROJ,
Ph.D.)

..... Thesis Advisor
(Professor JOONGJAI PANPRANOT, Ph.D.)

..... Examiner
(Associate Professor DEACHA CHATSIRIWECH, Ph.D.)

..... External Examiner
(Assistant Professor Okorn Mekasuwandumrong, D.Eng.)

กิตติธัช วงษ์เลขา : ผลของตัวรองรับไทเทเนียมและการเติมโคบอลต์ต่อตัวเร่งปฏิกิริยา
 Ni/TiO_2 ในปฏิกิริยาไฮโดรจิเนชันแบบเลือกเกิดของเฟอร์ฟูรัลเป็นเฟอร์ฟิวรัล
 แอลกอฮอล์. (EFFECTS OF TiO_2 SUPPORT AND Co ADDITION ON Ni/TiO_2
 CATALYSTS IN SELECTIVE HYDROGENATION OF FURFURAL TO
 FURFURYL ALCOHOL) อ.ที่ปรึกษาหลัก : ศ. ดร.จูงใจ ปั่นประณต

เฟอร์ฟิวรัลแอลกอฮอล์เป็นสารมัธยันตร์ที่มีความสำคัญในการผลิตโมเลกุลอนุพันธ์มูลค่าสูงที่สำคัญหลายชนิด โดยทั่วไปเฟอร์ฟิวรัลแอลกอฮอล์ผลิตจากปฏิกิริยาไฮโดรจิเนชันของเฟอร์ฟูรัลโดยใช้ตัวเร่งปฏิกิริยาโลหะที่มีตัวรองรับ งานวิจัยนี้เตรียม ๑๕ เปอร์เซ็นต์โดยน้ำหนักของนิกเกิลบนตัวรองรับไทเทเนียม (ไทเทเนียมไดออกไซด์) ด้วยวิธีการเคลือบฝัง โดยศึกษาผลของตัวรองรับไทเทเนียมที่มีองค์ประกอบเฟสและขนาดผลึกโดยเฉลี่ยต่างกัน และการเติมโคบอลต์ในปริมาณ ๑ ถึง ๓ เปอร์เซ็นต์โดยน้ำหนัก ต่อตัวเร่งปฏิกิริยา Ni/TiO_2 ในปฏิกิริยาไฮโดรจิเนชันแบบเลือกเกิดของเฟอร์ฟูรัลเป็นเฟอร์ฟิวรัลแอลกอฮอล์ที่ อุณหภูมิ ๕๐ องศาเซลเซียส ความดันไฮโดรเจน ๒๐ บาร์ และเวลาการทำปฏิกิริยา ๒ ชั่วโมง พบว่าโลหะนิกเกิลที่รองรับด้วยไทเทเนียมไดออกไซด์ที่มีองค์ประกอบเฟสผสมระหว่าง อนาเทสกับรูไทล์ ซึ่งมีขนาดผลึกและโครงสร้างของรูพูนที่เหมาะสม (Ni/TiO_2 -A2) ให้ค่าผลผลิตของเฟอร์ฟิวรัลแอลกอฮอล์ที่สูงที่สุดที่ ๔๓.๘๔ เปอร์เซ็นต์ โดยประสิทธิภาพในการเร่งปฏิกิริยาของตัวเร่งปฏิกิริยาสอดคล้องกับอันตรกิริยาระหว่างโลหะนิกเกิลกับไทเทเนียมไดออกไซด์ที่แข็งแรง และการกระจายตัวที่ดีของโลหะนิกเกิลบนตัวรองรับ การเติมโคบอลต์ลงในตัวเร่งปฏิกิริยานิกเกิลบนตัวรองรับไทเทเนียมไดออกไซด์ที่มีองค์ประกอบเฟสแบบ P25 และ A2 ทำให้ตัวเร่งปฏิกิริยาเหล่านี้วิบัติได้ง่ายขึ้น เป็นผลให้ความสามารถในการเร่งปฏิกิริยาของตัวเร่งปฏิกิริยาลดลง โดยที่ค่าการเลือกเกิดเป็นเฟอร์ฟิวรัลแอลกอฮอล์มีการเปลี่ยนแปลงเพียงเล็กน้อย

| | | |
|----------|--------------|----------------------------|
| สาขาวิชา | วิศวกรรมเคมี | ลายมือชื่อนิสิต |
| | | |
| ปี | 2561 | ลายมือชื่อ อ.ที่ปรึกษาหลัก |
| การศึกษา | | |

6070121421 : MAJOR CHEMICAL ENGINEERING

KEYWORD: Selective hydrogenation, Furfuryl alcohol, Furfural, Titanium dioxide,
Phase composition, Co addition

Kittithad Wonglekha : EFFECTS OF TiO₂ SUPPORT AND Co ADDITION ON
Ni/TiO₂ CATALYSTS IN SELECTIVE HYDROGENATION OF FURFURAL TO
FURFURYL ALCOHOL . Advisor: Prof. JOONGJAI PANPRANOT, Ph.D.

Furfuryl alcohol is an important chemical intermediate that can be converted into many value-added derivative molecules. It is typically produced by the hydrogenation of furfural using supported metal catalysts. In this work, 15%wt Ni catalysts supported on titania (TiO₂) were prepared by incipient wetness impregnation method. The effects of phase composition and average crystallite sizes of TiO₂ and Co addition in the range of 1-3 wt% on the catalytic properties of 15 wt%Ni/TiO₂ were investigated in the selective hydrogenation of furfural to furfuryl alcohol at 50°C, 20 bar of H₂, and 2 h reaction time. It was found that Ni supported on anatase-rutile mixed phase TiO₂ with appropriate crystallite size and pore structure (Ni/TiO₂-A2) exhibited the highest furfuryl alcohol yield at 43.84%. The catalytic performances of the catalysts corresponded to the relatively strong Ni-TiO₂ interaction and good dispersion of Ni on the support. Addition of Co into Ni/TiO₂ catalysts on P25 and A2 TiO₂ supports made the catalysts easier to be reduced and as a consequence, the catalyst activities decreased with little change on the FA selectivity.

Field of Study: Chemical Engineering Student's Signature

.....

Academic Year: 2018 Advisor's Signature

Year:

ACKNOWLEDGEMENTS

I really appreciate to my advisor Prof. Dr. Joongjai Panpranot for continuous support, suggestions, assistance, and encouragement until I made my thesis completed. She always helped me when I found problems with my research or writing. In addition, I would be grateful to Assoc. Prof. Anongnat Somwangthanaroj, as the chairman, Assoc. Prof. Deacha Chatsiriwech and Asst. Prof. Dr. Okorn Mekasuwandumrong as a member of the thesis committee and for your valuable comments and suggestions on this thesis.

Moreover, I would like to thank my parents and my friends for all their support and continuous encouragement throughout the period of this thesis.

Finally, I would like to acknowledge financial support from the Thailand Research Fund (BRG6180001 and RDG6150012).

Kittithad Wonglekha

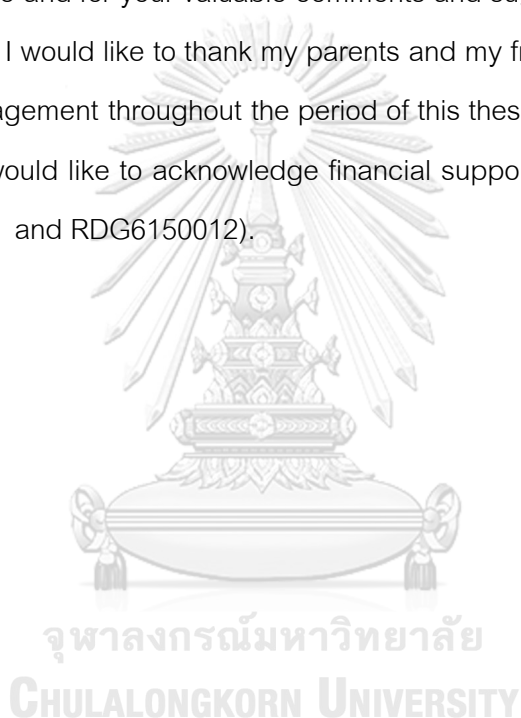


TABLE OF CONTENTS

| | Page |
|---|------|
| ABSTRACT (THAI)..... | iii |
| ABSTRACT (ENGLISH) | iv |
| ACKNOWLEDGEMENTS..... | v |
| TABLE OF CONTENTS..... | vi |
| LIST OF TABLES..... | ix |
| LIST OF FIGURES | xi |
| CHAPTER I INTRODUCTION..... | 1 |
| 1.1 Introduction | 1 |
| 1.2 Objectives of the Research | 2 |
| 1.3 Scopes of the Research..... | 3 |
| CHAPTER II BACKGROUND AND LITERATURE REVIEWS..... | 4 |
| 2.1 Hydrogenation Reaction | 4 |
| 2.2 Properties of nickel | 4 |
| 2.3 Study on TiO ₂ as a catalyst support | 5 |
| 2.4 Hydrogenation of furfural over heterogeneous catalyst | 7 |
| 2.5 The nickel-based catalyst on furfural hydrogenation | 15 |
| 2.6 Effect of Co-modified catalyst on catalyst properties and catalytic performance | 20 |
| CHAPTER III MATERIALS AND METHODS..... | 22 |
| 3.1 Materials | 22 |
| 3.2 Catalyst preparation..... | 24 |

| | |
|--|----|
| 3.2.1 Preparation of monometallic Ni/TiO ₂ catalysts by incipient wetness impregnation method..... | 24 |
| 3.2.2 Preparation of bimetallic Ni-Co/TiO ₂ catalysts by incipient wetness co-impregnation method..... | 25 |
| 3.3 Catalyst Characterization..... | 26 |
| 3.3.1 X-ray diffraction (XRD)..... | 26 |
| 3.3.2 N ₂ -physisorption..... | 26 |
| 3.3.3 Transmission electron spectroscopy (TEM)..... | 26 |
| 3.3.4 H ₂ -Temperature programmed reduction (H ₂ -TPR)..... | 26 |
| 3.3.5 X-ray photoelectron spectroscopy (XPS)..... | 26 |
| 3.3.6 H ₂ -pulse chemisorption..... | 27 |
| 3.4 Catalyst test in the furfural hydrogenation..... | 27 |
| 3.5 Research methodology..... | 30 |
| Part I. The investigation of the characteristics and catalytic performances of Ni nanoparticles supported on different phase composition and average crystallite sizes of TiO ₂ support in the liquid-phase furfural hydrogenation. | 30 |
| Part II. Study of the effect of bimetallic Ni-Co nanoparticles supported on different phase composition and average crystallite sizes of TiO ₂ support in liquid-phase furfural hydrogenation..... | 31 |
| CHAPTER IV RESULTS AND DISCUSSION..... | 32 |
| 4.1 Characterization of Ni/TiO ₂ with different phase compositions and average crystallite sizes of TiO ₂ support..... | 33 |
| 4.1.1 X-ray diffraction (XRD)..... | 33 |
| 4.1.2 N ₂ Physisorption..... | 35 |
| 4.1.3 H ₂ -temperature programmed reduction (H ₂ -TPR)..... | 37 |

| | |
|--|----|
| 4.1.4 Transmission electron spectroscopy (TEM) | 39 |
| 4.1.5 X-ray photoelectron spectroscopy (XPS)..... | 42 |
| 4.1.6 H ₂ -pulse Chemisorption (H ₂ -chem)..... | 45 |
| 4.2 Activity test in the liquid-phase furfural hydrogenation | 46 |
| 4.3 Characterization of Ni-Co/TiO ₂ with different Co contents | 50 |
| 4.3.1 X-ray diffraction (XRD)..... | 50 |
| 4.3.2 N ₂ Physisorption | 52 |
| 4.3.3 H ₂ -temperature programmed reduction | 54 |
| 4.3.4 X-ray photoelectron spectroscopy (XPS)..... | 55 |
| 4.3.5 H ₂ -pulse Chemisorption (H ₂ -chem)..... | 57 |
| 4.4 The catalytic performances of Ni/TiO ₂ and Ni-Co/TiO ₂ catalysts with different Co content in the liquid-phase furfural hydrogenation | 58 |
| CHAPTER V CONCLUSIONS..... | 60 |
| 5.1 Conclusions..... | 60 |
| 5.2 Recommendation | 60 |
| REFERENCES..... | 61 |
| APPENDIX A CALCULATION FOR CARALYST PREPARATION | 65 |
| APPENDIX B CALCULATION OF THE CRYSTALLITE SIZE | 67 |
| APPENDIX C CALCULATION OF THE PHASE COMPOSITION..... | 68 |
| APPENDIX D CALCULATION FOR METAL ACTIVE SITES AND DISPERSION | 69 |
| APPENDIX E CALCULATION FOR CATALYTIC PERFORMANCE | 71 |
| VITA | 74 |

LIST OF TABLES

| | page |
|---|------|
| Table 2.1 Physical properties of nickel | 5 |
| Table 2.2 Summary of the research of hydrogenation of furfural on various catalysts under different reaction conditions | 9 |
| Table 2.3 Summary of the research on the nickel-based catalyst on furfural hydrogenation with different supports and reaction conditions | 16 |
| Table 2.4 Physical properties of cobalt..... | 20 |
| Table 3.1 Chemicals used as precursors in catalyst preparation | 22 |
| Table 3.2 Chemicals used as supports in catalyst preparation | 22 |
| Table 3.3 Phase composition and crystallite size of supports in catalyst preparation | 24 |
| Table 3.4 Chemicals used in the liquid-phase furfural hydrogenation..... | 29 |
| Table 3.5 The operating conditions of gas chromatograph with a flame ionization detector | 29 |
| Table 4.1 The average crystallite sizes and %phase composition of the Ni/TiO ₂ catalysts with different phase compositions and average crystallite sizes | 34 |
| Table 4.2 The physical properties of the Ni/TiO ₂ catalysts with different phase compositions and average crystallite sizes | 37 |
| Table 4.3 The surface atomic composition of the Ni/TiO ₂ catalysts with different phase compositions and average crystallite sizes | 43 |
| Table 4.4 The H ₂ chemisorption and metal concentrations of the Ni/TiO ₂ catalysts with different phase compositions and average crystallite sizes..... | 46 |
| Table 4.5 The catalytic performances of Ni/TiO ₂ catalysts with different phase compositions and average crystallite sizes | 49 |
| Table 4.6 The average crystallite sizes and %phase composition of the Ni/TiO ₂ -A2 and Ni-Co/TiO ₂ catalysts with different Co contents | 51 |
| Table 4.7 The physical properties of the Ni/TiO ₂ -A2 and Ni-Co/TiO ₂ catalysts with different Co contents | 54 |

| | page |
|---|------|
| Table 4.8 The H ₂ chemisorption and metal concentrations of the Ni/TiO ₂ -A2 and Ni-Co/TiO ₂ catalysts with different Co contents..... | 57 |
| Table 4.9 The catalytic performances of Ni/TiO ₂ -A2 and Ni-Co/TiO ₂ -A2 catalysts with different Co contents | 59 |
| Table 4.10 The catalytic performances of Ni/TiO ₂ -P25 and Ni-2%Co/TiO ₂ -P25 catalysts | 59 |



LIST OF FIGURES

| | page |
|--|------|
| Figure 2.1 The applications of furfuryl alcohol..... | 8 |
| Figure 2.2 The hydrogenation pathway of furfural | 8 |
| Figure 2.3 The side reaction product from using methanol as a solvent | 9 |
| Figure 3.1 Diagram of Ni on TiO ₂ catalysts preparation by incipient wetness impregnation method | 25 |
| Figure 3.2 Diagram of Ni-Co on TiO ₂ catalysts preparation by incipient wetness co- impregnation method | 26 |
| Figure 3.3 Schematic of the liquid-phase hydrogenation of furfural | 29 |
| Figure 4.1 The XRD patterns of Ni/TiO ₂ catalysts with different phase compositions and average crystallite sizes | 34 |
| Figure 4.2 N ₂ -physisorption isotherms of Ni/TiO ₂ -P25, Ni/TiO ₂ -A1, Ni/TiO ₂ -A2, Ni/TiO ₂ -R1, and Ni/TiO ₂ -R2..... | 35 |
| Figure 4.3 The combination of N ₂ -physisorption isotherms of Ni/TiO ₂ -P25, Ni/TiO ₂ -A1, Ni/TiO ₂ -A2, Ni/TiO ₂ -R1, and Ni/TiO ₂ -R2..... | 36 |
| Figure 4.4 H ₂ -TPR profiles of Ni/TiO ₂ catalysts with different phase compositions and average crystallite sizes | 38 |
| Figure 4.5 TEM images of the Ni/TiO ₂ catalysts: (a) Ni/TiO ₂ -A1; (b) Ni/TiO ₂ -A2; (c) Ni/TiO ₂ -P25; (d) Ni/TiO ₂ -R1; and (e) Ni/TiO ₂ -R2..... | 39 |
| Figure 4.6 Ni 2p peak in XPS spectra of Ni/TiO ₂ with catalysts with different phase compositions and average crystallite sizes | 44 |
| Figure 4.7 The pathways of furfural hydrogenation reaction | 46 |
| Figure 4.8 The XRD patterns of Ni/TiO ₂ -A2 and Ni-Co/TiO ₂ -A2 catalysts with different Co contents | 50 |
| Figure 4.9 The N ₂ -physisorption isotherms of Ni/TiO ₂ -A2, Ni-1%Co/TiO ₂ -A2, Ni- 2%Co/TiO ₂ -A2, Ni-3%Co/TiO ₂ -A2, and Ni-2%Co/TiO ₂ -P25 | 52 |
| Figure 4.10 Combination of N ₂ -physisorption isotherms of Ni/TiO ₂ -A2 and Ni-Co/TiO ₂ catalysts..... | 53 |

| | page |
|---|------|
| Figure 4.11 The H ₂ -TPR profiles of Ni/TiO ₂ -A2 and Ni-Co/TiO ₂ -A2 catalysts with different Co contents | 55 |
| Figure 4.12 Ni 2p peak in XPS spectra of Ni/TiO ₂ -A2 and Ni-Co/TiO ₂ -A2 catalysts with different Co contents | 56 |
| Figure E.1 The calibration curve of furfural | 70 |
| Figure E.2 The calibration curve of furfuryl alcohol | 70 |
| Figure E.3 The calibration curve of tetrahydrofurfuryl alcohol..... | 71 |



CHAPTER I

INTRODUCTION

1.1 Introduction

Because of the utilization of fossil fuels has been increased, humanity is confronted with the problems of an energy crisis and environmental pollution [1]. Nowadays, the research is focused on the development of strategies for transforming renewable biomass, which is an ideal renewable resource, into fuels and chemicals [2]. Furfural is a biomass-derived chemical, received by acid-catalyzed dehydration of xylose, the main building-block of hemicellulose constituent of lignocellulose [3]. Furfural is currently considered as one of the most important biomass-derived chemicals that are available in large volume and high versatility [4]. It can be converted into a wide range of value-added derivative molecules, which can be used as plasticizers, solvents, agrochemicals, monomers in the production of resins (e.g., furfuryl alcohol (FA) and tetrahydrofurfuryl alcohol (THFA)) [5]. Furfuryl alcohol (FA) is the most common hydrogenation product of furfural, with 62% of furfural produced being transformed into furfuryl alcohol. FA is an important chemical intermediate widely used in the polymer industry and in the fine chemical industry [6].

In the present industrial processes, copper chromite catalysts are used in the selective hydrogenation of furfural to FA. Although copper chromate catalysts exhibit good activity, selectivity, and stability, copper chromite catalysts are their high toxicity, which can cause serious environmental pollution [1]. Therefore, the design of Cr-free catalysts is interest for the FA production from furfural hydrogenation. Most of the researches have been investigated using various supported metals as catalysts, including precious metal catalysts (Pt, Pd, Rh, and Ru) and nonprecious metal catalysts (Cu, Ni, and Co). Precious metal catalysts showed high catalytic performance for the

selective hydrogenation of furfural to FA, but they have limited availability and high cost. As a result, there is increased interest in nonprecious metal catalysts [1, 2].

Therefore, improving catalytic performance of the metal catalysts was investigated by using promoters, tuning particle sizes, varying supports and modifying the active metal with second metals [7-10]. The significant factor that showed a large effect on catalytic performance is modifying the active metal with a second metal to form a bimetallic catalyst. In Ni-based catalysts, the addition of a second metal, such as Co or Cu, increases the selectivity for the hydrogenation of various unsaturated carbonyls [11, 12]. For example, Saranya A. et al., [11] reported that Ni-Co catalysts exhibited higher selectivity towards C=O hydrogenation than monometallic Ni catalysts in the cinnamaldehyde hydrogenation reaction. The addition of Co to Ni may be able to improve the selectivity of C=O hydrogenation to produce FA.

In this work, Ni/TiO₂ were prepared by impregnation methods and tested in the selective hydrogenation of furfural to FA. The effect of phase composition and average crystallite sizes of TiO₂ supports (P25, rutile(R1), rutile(R2), anatase(A1) and anatase(A2)) on the catalytic properties were investigated by several characterization techniques X-ray diffraction (XRD), N₂-physisorption, transmission electron microscopy (TEM), H₂-temperature programmed reduction (H₂-TPR), and X-ray photoelectron spectroscopy (XPS) and H₂-pulse chemisorption.

1.2 Objectives of the Research

1. To investigate the characteristics and catalytic properties of Ni/TiO₂ catalysts prepared by impregnation methods with different phase composition and average crystallite sizes of TiO₂ in the selective hydrogenation of furfural to furfuryl alcohol.

2. To study the effect of bimetallic Ni-Co nanoparticles supported on different phase composition and average crystallite sizes of TiO_2 in the selective hydrogenation of furfural to furfuryl alcohol.

1.3 Scopes of the Research

1. Titanium dioxide support with different phase composition and average crystallite sizes (P25, rutile(R1), rutile(R2), anatase(A1) and anatase(A2)) were used without further purification.
2. 15 wt% Ni/ TiO_2 monometallic catalysts with different phase composition and average crystallite sizes of TiO_2 supports were prepared by incipient wetness impregnation method and calcined at 500°C under air atmospheres for 2 h.
3. The bimetallic catalysts of 15 wt% Ni with different amounts of Co (1, 2, 3 wt%) supported on different phase composition and average crystallite sizes of TiO_2 supports were prepared by incipient wetness co-impregnation method and calcined at 500°C under air atmospheres for 2 h.
4. The catalysts were reduced under H_2 flow (25 ml/min) at 500°C for 3 h.
5. The catalysts were tested in the liquid phase furfural hydrogenation in a batch reactor at constant temperature 50°C and pressure 20 bar of hydrogen pressure for 2 h.
6. The catalysts were characterized by various methods including
 - 6.1 X-ray diffraction (XRD)
 - 6.2 N_2 -physisorption
 - 6.3 Transmission electron microscopy (TEM)
 - 6.4 Hydrogen Temperature-programmed reduction (H_2 -TPR)
 - 6.5 X-ray photoelectron spectroscopy (XPS)
 - 6.6 H_2 -pulse chemisorption (H_2 -chem)

CHAPTER II

BACKGROUND AND LITERATURE REVIEWS

2.1 Hydrogenation Reaction

The hydrogenation reaction is a chemical reaction between a hydrogen molecule and other compounds. This process is considered as one of the crucial reactions and widely used for chemical synthesis of organic compounds in pharmaceuticals, agrochemicals, food industry, and in the petrochemical industry. The reaction typically is used with catalysts, which is called catalytic hydrogenation. Catalysts in this reaction can be both heterogeneous and homogeneous catalysts.

Normally, the mechanism of homogeneous catalysts is directly interacted at reactants and catalysts and is easier than heterogeneous catalysts, but the homogeneous catalysts are the soluble catalysts or it performs in the same phase as the reactants, so the separation of these catalysts from products is difficult and expensive. In contrast, the heterogeneous catalysts have different phases from the reactants, so it easily provides separation from the products. Moreover, the heterogeneous catalysts have better thermal stability than the homogeneous catalysts [13].

2.2 Properties of nickel

Nickel is a chemical element with symbol Ni and atomic number 28. It is a silvery-white lustrous, hard, and ductile metal. It is one of four elements that are ferromagnetic at or near room temperature. Nickel is typically composed of five isotopes; ^{58}Ni , ^{60}Ni , ^{61}Ni , ^{62}Ni , ^{64}Ni , which ^{58}Ni is the most abundant. At room temperature, Nickel is slowly oxidized by air, so it is considered as a corrosion-resistant. It was used in many applications, such as plating iron and brass, coating chemistry equipment, and manufacturing certain alloys [14]. Physical properties of nickel are shown in Table 2.1.

Table 2.1 Physical properties of nickel [15]

| Physical Properties | |
|------------------------|--------------------------------------|
| Atomic number | 28 |
| Atomic weight | 58.7 |
| Electron configuration | [Ar] 3d ⁸ 4s ² |
| Electronegativity | 1.91 |
| Crystal structure | Face centered cubic (fcc) |
| Melting point | 1728 K (1455°C) |
| Boiling point | 3003 K (2730°C) |
| Density @ 293K (20°C) | 8.91 g/cm ³ |

2.3 Study on TiO₂ as a catalyst support

Titanium dioxide (TiO₂), which is known as titania, has chemical formula TiO₂. It has been widely utilized in mineralizing toxic and non-biodegradable environmental contaminants because of its nontoxicity, long-term photo stability, and high effectiveness. Moreover, it has a good mechanical resistance and stabilities in acidic and oxidative environments. From these properties, TiO₂ is a prime candidate for heterogeneous catalyst support. Therefore, it is widely used as an interesting support material for metals or metal oxides due to its ability to modify the catalytic properties of the supported phase. It exists in three main structures: anatase, rutile, and brookite.

Anatase and rutile are the most common structures, but the crystalline size of the rutile is always larger than the anatase phase. Brookite is infrequently utilized. Generally, Rutile phase is the only stable phase, whereas anatase and brookite phases can be transformed to rutile phase at above 600°C. Metal supported on titania with different structures might exhibit different physicochemical properties and catalytic properties as a result of metal-TiO₂ support interaction (SMSI) [16, 17].

Jongsomjit et al. (2005) [18] studied the Co supported on various ratios of rutile: anatase in titania prepared by incipient wetness impregnation method. The catalytic performances of catalysts were tested in CO hydrogenation. They found that both activity and selectivity of Co/TiO₂ catalysts in CO hydrogenation were affected by changing the anatase/rutile ratios in TiO₂ support that influenced the metal cobalt surface, the reason of which was not given.

Na Y et al. (2008) [19] studied the TiO₂-supported Ni catalysts prepared by incipient wetness impregnation method. Pure anatase titania was used as support but was calcined at different temperatures (773 K to 1173 K). Activity and selectivity of the catalysts were evaluated in liquid phase hydrogenation of o-chloronitrobenzene. They found that calcination temperature had a great influence on the physicochemical properties of Ni/TiO₂ catalysts. When calcination temperature is increased, the specific surface area and the pore volume of the catalysts decreased and NiO-TiO₂ interaction became weak. The reactivity of Ni/TiO₂ catalysts in the hydrogenation is associated with nickel active area and metal support interaction (SMSI).

K. Joseph Antony Raj et al. (2012) [20] studied the Ni supported on various phases of titania, viz. rutile, anatase and high surface area (TiO₂) prepared by impregnation method and calcined at two different temperatures, 500°C and 900°C. Moreover, they investigated the optimum condition. Catalytic performances of the catalysts were evaluated in liquid phase selective hydrogenation of acetophenone. They

found that the Ni content of 15 wt%, a hydrogen pressure of 40 kg/cm² and the reaction temperature of 140°C were optimum to achieve good conversion of acetophenone. The samples calcined at 500°C showed higher activity than those calcined at 900°C. Ni/rutile that calcined at 500°C showed higher activity than other catalysts because it had a higher concentration of Ni on the surface of rutile and strong metal support interaction (SMSI) between rutile and Ni than that between Ni and anatase or TiO₂.

2.4 Hydrogenation of furfural over heterogeneous catalyst

Furfural, produced by the acid-catalyzed dehydration or hydrolysis of xylose, is a versatile and renewable chemical. It was widely used in many industrial applications including fragrance, agrochemical and plastics industries. The hydrogenation of furfural to furfuryl alcohol (FA) is a single step process in liquid or vapor phase by the heterogeneous catalysis reaction. Approximately 60–62% of the furfural that produced worldwide was converted to furfuryl alcohol (FA). Furfuryl alcohol is used in the production of synthetic fibres and resins in the polymer industry. It is used in the manufacture of vitamin C, lubricants and a chemical building block for drug synthesis. It is also used in the fine chemical industry [20]. The applications of furfuryl alcohol are shown in **Figure 2.1**. The hydrogenation of furfural consists of two functional groups, which are C=C double bond and C=O double bond. Therefore, many products are formed via furfural hydrogenation with a variety of side reactions that performed in **Figure 2.2** including decarbonylation and oxidation also possible. However, the reaction was operated with organic solvents such as methanol and ethanol. The side reaction product may be occurred from using some of the solvents. For example, when methanol was used as a solvent, 2-furaldehyde dimethyl acetal, which was called solvent product (SP), may be formed as shown in **Figure 2.3** [21].

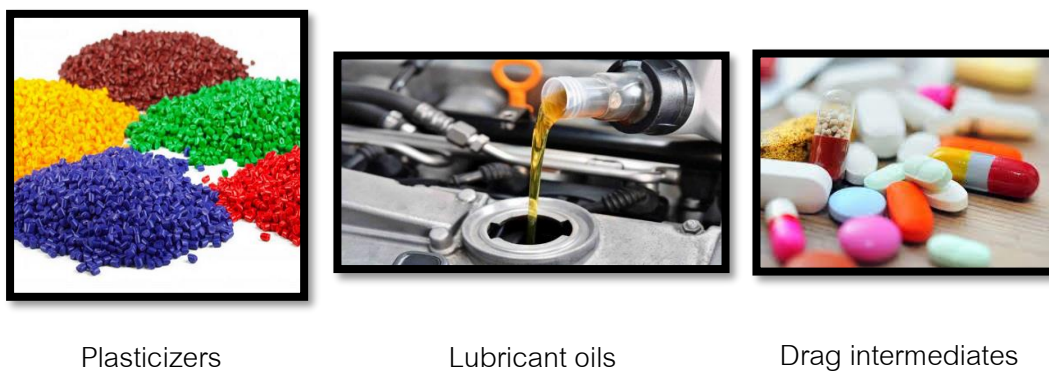


Figure 2.1 The applications of furfuryl alcohol

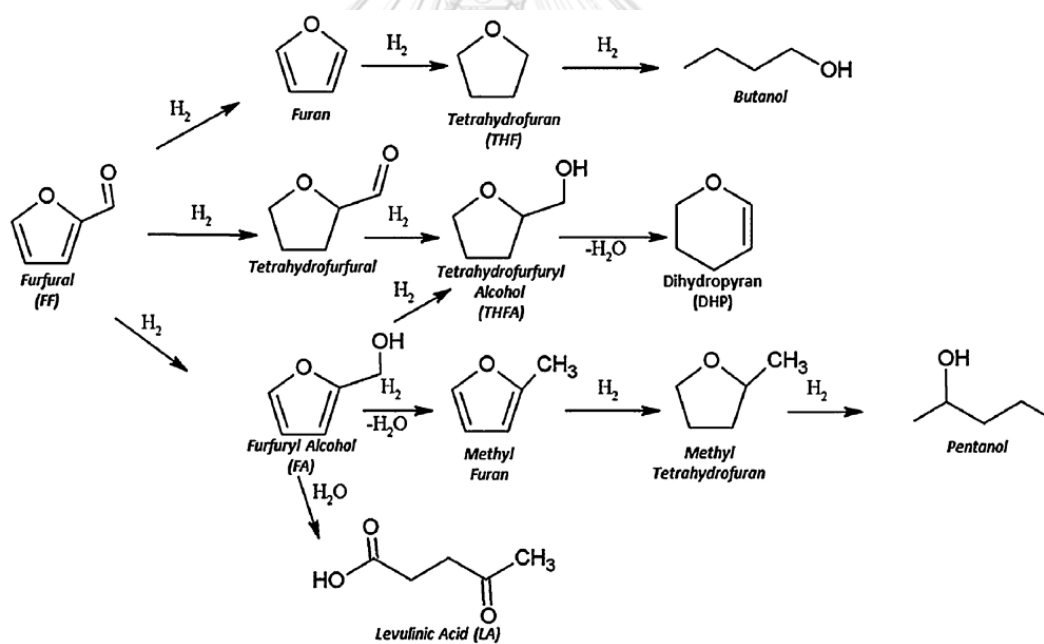


Figure 2.2 The hydrogenation pathway of furfural [21]

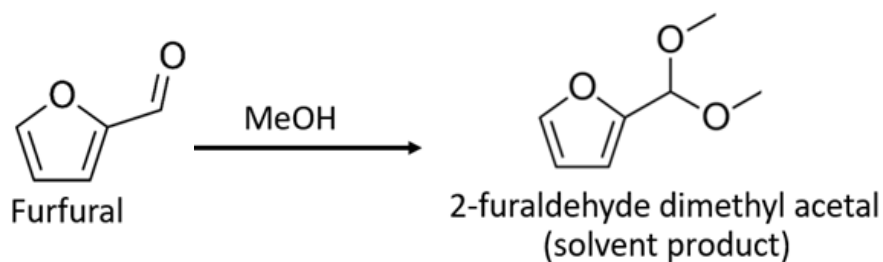


Figure 2.3 The side reaction product from using methanol as a solvent [22]

Summary of the research of furfural hydrogenation on various catalysts under different reaction condition is shown in Table 2.2.

Table 2.2 Summary of the research of hydrogenation of furfural on various catalysts under different reaction conditions

| Researcher | Purposes of study | Catalyst and preparation method | Reaction condition | Results |
|---|--|---|---|---|
| Vargas-Hernández, D. et al. (2014) [23] | Studied Cu supported on SBA-15 silica catalysts and compared Catalytic | Cu/SBA-15 silica with 8, 15, 20 wt% Cu loading) were prepared by impregnation | -Vapor phase -Calcined at 400°C for 6h -Reduced at 350°C for 2h | - 15%wt Cu/SBA-15 catalyst shows the highest activity and selectivity at 170°C under this condition -All Cu/SBA-15 catalysts have more long term stability than copper |

| | | | | |
|--------------------------------------|--|---|--|---|
| | behavior with copper chromite for the hydrogenation of furfural to furfuryl alcohol | | -Catalyst 150 mg, T = 170°C, H ₂ flow 10 ml/min, Reaction time = 5 h | chromite |
| Bhogeswara rao, S. et al. (2015) [3] | Studied γ -Al ₂ O ₃ supported Pt and Pd catalysts in the selective liquid phase hydrogenation of furfural to furfuryl alcohol | Pt/ γ -Al ₂ O ₃ and Pd/ γ -Al ₂ O ₃ were prepared by wet impregnation method. | -Liquid phase -Calcined at 400°C for 2h -Pd Reduce at 250°C for 2.5h -Pt Reduce at 350°C for 2.5h | -At T 25°C, Pt catalysts were selective of C=O group but Pd catalysts hydrogenated both ring and C=O groups. - At higher temperature (T ≥ 180°C), Pd catalysts enabled decarbonylation of furfural giving furan 82% yield. |

| | | | | |
|--|--|--|---|--|
| | | | <p>-Catalyst 50 mg, T=25°C and ≥180 °C P_{H₂}=20 atm Reaction time = 8 h</p> | |
| <p>Taylor, M.J. et al. (2016) [22]</p> | <p>Studied Pt nanopartic le supported on SiO₂, ZnO, Y- Al₂O₃, CeO₂ with different solvents in the selective liquid</p> | <p>Pt/SiO₂, Pt/ZnO, Pt/Y-Al₂O₃, Pt/CeO₂ were prepared by adapting the method of Jones et al.</p> | <p>-Liquid phase -Calcined at 300°C for 4h -Reduced at 200°C for 1h -Catalyst 20 mg, T = 50°C</p> | <p>-Pt/Y-Al₂O₃ showed the highest catalytic performances in methanol with furfural conversion 80% and furfuryl alcohol selectivity 99%</p> |

| | | | | |
|-----------------------------|---|---|---|---|
| | phase hydrogenation of furfural to furfuryl alcohol under mild conditions. | | $P_{H_2} = 1$ atm Reaction time = 7 h | |
| Zhang, C. et al. (2017) [4] | Studied the effect of bimetallic overlayer catalysts (Ni-Pt/SiO ₂ and Cu-Pt/SiO ₂) and compared with monometallic catalysts (Ni/SiO ₂ , Cu/SiO ₂ , | Ni-Pt/SiO ₂ and Cu-Pt/SiO ₂ were synthesized using incipient wetness impregnation Ni@Pt/SiO ₂ and Cu@Pt/SiO ₂ were prepared by directed deposition technique. | -Liquid phase -Reduced at 400°C for 3h -Catalyst 0.1-0.3 g, T = 250°C $P_{H_2} = 6.8$ atm Reaction time = 1.5 h | -Ni@Pt/SiO ₂ and Cu@Pt/SiO ₂ overlayer catalysts showed higher reactivity in furfural conversion compared to their parent metals. -Cu@Pt overlayer catalyst showed high furfuryl alcohol selectivity |

| | | | | |
|---------------------------------------|--|--|--|---|
| | Pt/SiO ₂) for furfural hydrogena tion. | | | |
| Musci, J. J. et al. (2017) [24] | Studied the effect of Sn adding in carbon- supported monometal lic Ru and varied Sn/Ru ratio for aqueous phase hydrogena tion of furfural | Ru/C and RuSn/C were prepared by impregnation method | -Liquid phase -Activated at 300°C for 2h -Catalyst 250 g, T=90°C P _{H₂} =1.25 MPa Reaction time = 5 h | RuSn0.4/C (Sn/Ru ratio = 0.4) catalyst showed the highest catalytic performance both of furfural conversion at 91 % and furfuryl alcohol selectivity at 90% |

Vargas-Hernández, D. et al. (2014) [23] studied the effects of the Cu supported on SBA-15 silica catalysts with various Cu loadings (8, 15, and 20 wt%) in vapor phase furfural hydrogenation and they also compared these catalysts with copper chromite. Moreover, they investigated the effect of different experimental parameters, such as

catalyst loading, reaction temperature, the weight of catalyst and furfural feed, on the catalytic performance. From the result, they found that the presence of $\text{Cu}^0\text{-Cu}^+$ species on the catalyst surface is responsible for the high activity and selectivity toward furfuryl alcohol. The SBA-15Cu showed high catalytic performance toward the desired product at 170 °C. From the comparison between all the SBA-15 silica catalysts and copper chromite, it found that all the SBA-15 silica catalysts showed higher activity than copper chromite because of more long term stability.

Bhogeswararao, S. et al. (2015) [3] studied the effect of temperatures and concentration of metal loadings of $\gamma\text{-Al}_2\text{O}_3$ -supported Pt and Pd catalysts in furfural hydrogenation. At 25°C, they found that the supported Pt catalysts were only hydrogenated C=O groups of furfural to produce furfuryl alcohol, but the supported Pd catalysts hydrogenated both ring and C=O groups to produce tetrahydrofurfuryl alcohol and furfuryl alcohol). At higher temperatures reaction, the supported Pd catalysts enabled decarbonylation of furfural forming furan in 82% yield. In addition, the supported Pt catalysts promoted hydrogenolysis of C=O and C-O groups enabling 2-methylfuran and furan ring-opened products.

Taylor, M. J. et al. (2016) [22] studied the effect of the supported Pt catalysts with different support (SiO_2 , ZnO, $\gamma\text{-Al}_2\text{O}_3$, CeO_2 , and MgO) and the effect of varying solvents of reaction (polar solvent and nonpolar solvent) in the selective hydrogenation of furfural to furfuryl alcohol under extremely mild reaction conditions. From the result, they found that furfural hydrogenation was sensitive to Pt particle size. The particle size of Pt, which is approximately 4 nm, had high activity and selectivity in the hydrogenation reaction when used methanol as a solvent. Although the 4 nm of Pt size gave good catalytic performances, the results depended on the support of catalyst. They also found that this reaction is sensitive to the solvent used. From varying solvents, it showed

that alcohols solvent is more active than non-polar solvents. In addition, they found that some of the solvents can cause a side reaction to form side reaction product.

Zhang, C. et al. (2017) [4] studied the effect of bimetallic overlayer catalysts (Ni@Pt/SiO_2 and Cu@Pt/SiO_2) comparison with monometallic catalysts (Ni/SiO_2 , Cu/SiO_2 , Pt/SiO_2) in furfural hydrogenation. From the result, they found that Cu@Pt and Ni@Pt catalysts showed higher reactivity compared to their parent metals due to reducing binding strength of H_2 on the Pt surface. It caused fewer Pt sites being blocked by strong H_2 adsorption and increased Pt reactivity.

Musci, J. J. et al. (2017) [24] studied the effect of Sn adding in carbon-supported monometallic Ru and effect of the Sn/Ru atomic ratio (0, 0.1, 0.2, 0.4 and 0.8) in aqueous phase hydrogenation of furfural at 90 °C and 1.25 MPa. They found that the adding amount of Sn to Ru catalyst could improve the efficiency of the catalyst. They also found that the Sn/Ru ratio of 0.4 promoted the C=O hydrogenation reaching a selectivity towards furfuryl alcohol. However, when adding more Sn at higher concentration, the reaction results were not improved. It seems to be a compromise between the dilution of Ru sites, active for the hydrogenation reaction, and the promoter effect of Sn.

2.5 The nickel-based catalyst on furfural hydrogenation

Supported nickel catalysts have been widely used in many hydrogenation reactions due to their high reactivity, easy availability, and lower price. Summary of the research of furfural hydrogenation on various catalysts under different reaction condition is shown in **Table 2.3**.

Table 2.3 Summary of the research on the nickel-based catalyst on furfural hydrogenation with different supports and reaction conditions.

| Researcher | Purposes of study | Catalyst and preparation method | Reaction condition | Results |
|-----------------------------------|--|---|--|--|
| Lujie, L et al. (2016) [25] | Studied the Ni, Cu and bimetallic Cu-Ni with different metals loadings supported on CNTs and the effect of various reaction parameters in the selective hydrogenation of | Ni/CNT, Cu/CNT, Cu-Ni/CNT, were prepared by impregnation method | -Liquid phase -Reduced at 400°C for 4h -Catalyst 0.1 g, T = 130°C, P _{H₂} = 40 bar Reaction time = 10 h | - 10 wt%Ni/CNT and Cu-Ni/CNT with mole ratio 1:1 showed good catalytic performance |

| | | | | |
|-------------------------------|--|--|--|---|
| | furfural to tetrahydrofurfuryl alcohol | | | |
| Zhaolin F. et al. (2017) [26] | Studied the Ni, Cu and bimetallic Ni-Cu supported on Al ₂ O ₃ with formic acid as a hydrogen donor in the selective hydrogenation of furfural to 2-methylfuran | Ni/ Al ₂ O ₃ , Cu/ Al ₂ O ₃ , Ni-Cu/ Al ₂ O ₃ , were prepared by incipient wetness impregnation method | -Liquid phase -Calcined at 500°C for 5h - Cu/ Al ₂ O ₃ reduce at 400°C for 2h - Ni/ Al ₂ O ₃ and Ni-Cu/ Al ₂ O ₃ reduce at 550°C for 2h -Catalyst 0.15 g, T=210°C P _{H₂} =1 | - Ni-10%Cu/Al ₂ O ₃ exhibited better catalytic performances than both mono metal catalysts - With the increase of Ni content in Ni-10%Cu/Al ₂ O ₃ , the catalyst turned more active and more selective to the formation of 2-methylfuran - The solvent and the amount of formic acid that was used in reaction were influential for the reduction process |

| | | | | |
|-----------------------------|---|---|---|--|
| | | | MPa Reaction time = 7 h | |
| Pei J. et al. (2018) [1] | Studied the Ni, Cu, Co, and Fe and bimetallic Ni-based supported on SiO ₂ with different solvents in the selective hydrogenation of furfural to furfuryl alcohol | -monometallic catalysts were prepared by impregnation method - bimetallic catalysts were prepared by coimpregnation method | -Liquid phase -Calcined at 450°C for 3h -Reduced at 450°C for 3h -Catalyst 1.2 g, T = 140°C P _{H2} = 3.4 MPa Reaction time = 5 h | - The addition of Fe to the Ni catalyst enhances both the activity and selectivity -The liquid-phase selective hydrogenation of furfural is sensitive to the solvent used - Ni ₃ Fe ₁ /SiO ₂ catalyst using methanol as solvent showed the best catalytic results |

Lujie, L et al. (2016) [25] studied the supported Ni, Cu and bimetallic Cu-Ni with different metals loadings supported on CNTs and the effect of various reaction parameters in the selective hydrogenation of furfural to tetrahydrofurfuryl alcohol. From the result, they found that bimetallic synergistic effect in Cu-Ni/CNT catalysts could improve the catalytic selectivity of this reaction. The 10 wt% Ni/CNT and bimetallic catalysts with Cu-Ni with mole ratio 1:1 showed the high conversion of furfural and selectivity towards tetrahydrofurfuryl alcohol. They also found the possible mechanism of hydrogen-transfer for the hydrogenation of furfural to tetrahydrofurfuryl alcohol.

Zhaolin F. et al. (2017) [26] studied the supported Ni, Cu and bimetallic Ni-Cu supported on Al_2O_3 with formic acid as a hydrogen donor in the selective hydrogenation of furfural to 2-methylfuran. From the result, they found that the $\text{Ni}/\text{Al}_2\text{O}_3$ showed a high catalytic activity both in decarbonylation and hydrogenation, so it caused a moderate selectivity to 2-methylfuran. Contrarily, the $\text{Cu}/\text{Al}_2\text{O}_3$ showed a low catalytic activity but a high selectivity for the hydrogenation of carbonyl. The $\text{Ni-10\%Cu}/\text{Al}_2\text{O}_3$ exhibited better catalytic performances than both $\text{Ni}/\text{Al}_2\text{O}_3$ and $\text{Cu}/\text{Al}_2\text{O}_3$ catalysts. When the addition of Ni content in $\text{Ni-10\%Cu}/\text{Al}_2\text{O}_3$ was increased, the catalyst can improve activity and selectivity to form 2-methylfuran. They also found that the reaction solvent and the addition amount of formic acid were influential for the reduction process.

Pei J. et al. (2018) [1] studied the supported Ni, Cu, Co, and Fe and bimetallic Ni-based supported on SiO_2 with different solvents in the selective hydrogenation of furfural to furfuryl alcohol. From the result, they found that the addition of Fe to the Ni catalyst enhances both the activity and selectivity for the hydrogenation of furfural to furfuryl alcohol (FFA). The optimum Ni/Fe atomic ratio is 3:1. They also found that the liquid-phase selective hydrogenation of furfural is sensitive to the solvent used. Protic solvents, especially alcohols, showed the highest activity and FFA selectivity.

Tetrahydrofurfuryl alcohol, which is produced from the side reaction, was almost completely inhibited due to competitive adsorption when using methanol as solvent.

2.6 Effect of Co-modified catalyst on catalyst properties and catalytic performance

Cobalt is a chemical element with symbol Co and atomic number 27. It is a brittle, hard, lustrous, silver-gray metal. It is one of four elements that are ferromagnetic at or near room temperature. Cobalt has +2 and +3 of common oxidation states from ranging -3 to +5. Cobalt has a high melting point and is hard-wearing at high temperature. From all of the properties, cobalt is primarily used in the manufacture of magnetic, wear-resistant and high-strength alloys. Its alloys were used in high-speed steels and cutting tools for instance [27]. Physical properties of cobalt are shown in Table 2.4.

Table 2.4 Physical properties of cobalt [28]

| Physical Properties | |
|------------------------|--------------------------------------|
| Atomic number | 27 |
| Atomic weight | 58.9 |
| Electron configuration | [Ar] 3d ⁷ 4s ² |
| Electronegativity | 1.88 |
| Crystal structure | hexagonal close packed (hcp) |
| Melting point | 1768 K (1495°C) |
| Boiling point | 3203 K (2930°C) |
| Density @ 293K (20°C) | 8.90 g/cm ³ |

Zheng, R. et al. (2012) [29] studied the SiO_2 supported Co, Cu, Pt monometallic catalysts and the SiO_2 supported Co-Pt and Cu-Pt bimetallic catalysts in liquid phase hydrogenation of cinnamaldehyde. From the results, they found that CO chemisorption results showed that Co-Pt had significantly higher CO chemisorption capacity than monometallic catalysts. They also found that Co-Pt and Cu-Pt bimetallic catalysts exhibited more hydrogenation activity than the corresponding monometallic catalysts. In addition, Co-Pt bimetallic catalysts showed much higher selectivity toward C=O bond hydrogenation than Cu-Pt.

Saranya A. et al. (2018) [11] studied the effects of the bimetallic Co-Ni supported on TiO_2 -P25 catalysts with various composition range $\text{Co}_{(1-x)}\text{Ni}_x$ ($x = 0.0, 0.2, 0.3, 0.4, 0.5, 0.6, 0.8, \text{ and } 1.0$) in the selective hydrogenation of cinnamaldehyde. From the results, they found that the bimetallic Co-Ni catalysts in the composition range $x = 0.3\text{--}0.6$ showed the very high conversion of cinnamaldehyde (CAL) at 98%. Bimetallic $\text{Co}_{0.7}\text{Ni}_{0.3}$ catalyst displayed high conversion of CAL and high selectivity towards hydrocinnamyl alcohol (HCOL) at 98.1 and 82.9, respectively. The $\text{Co}_{0.5}\text{Ni}_{0.5}$ catalyst exhibited a maximum value of TOF. Moreover, they also found that the Co-Ni alloy formation can improve the electronic structure, d-band characteristics, and metal-H bond strength, so it is responsible for the observed changes in activity and selectivity. A synergetic effect, which is originated from an appropriate composition of Co and Ni and reaction conditions, had highly effective to non-noble metal base catalysts for hydrogenation reactions, in comparison with noble metal-based catalysts.

CHAPTER III

MATERIALS AND METHODS

This chapter explains the detail about experimental of this research including materials, catalyst preparation, catalyst characterization, catalyst test, and research methodology in the selective hydrogenation of furfural.

3.1 Materials

The chemicals that used as precursors and supports for catalyst preparation by were shown in **Table 3.1** and **Table 3.2**, respectively.

Table 3.1 Chemicals used as precursors in catalyst preparation

| Chemicals | Formula | Suppliers |
|-----------------------------------|--|----------------------|
| Nickel(II) nitrate hexahydrate | $\text{Ni}(\text{NO}_3)_2 \cdot 6\text{H}_2\text{O}$ | Merck KGaA |
| Cobalt(II) nitrate hexahydrate | $\text{Co}(\text{NO}_3)_2 \cdot 6\text{H}_2\text{O}$ | Aldrich Chemical Ltd |

Table 3.2 Chemicals used as supports in catalyst preparation

| Product code | Chemical | Symbol | Suppliers |
|-------------------------------|--|--------|-------------------------|
| - | P25 | P25 | DEGUSSA |
| 637262 (TiO ₂) | Titanium(IV) oxide, rutile nanopowder, <100 nm particle size, 99.5% trace metals basis | R1 | Aldrich Chemical Ltd |
| 224227 (TiO ₂) | Titanium(IV) oxide, rutile powder, <5 μm, ≥99.9% trace metals basis | R2 | Aldrich Chemical Ltd |

| | | | |
|-------------------------------|--|----|----------------------|
| 637254 (TiO ₂) | Titanium(IV) oxide, anatase nanopowder, <25 nm particle size, 99.7% trace metals basis | A1 | Aldrich Chemical Ltd |
| 45603 (TiO ₂) | Titanium(IV) oxide, anatase nanopowder 15 nm, 99.7% (metals basis) | A2 | Alfa Aesar |

The phase composition and crystallite size of supports that used in the catalyst preparation as shown in Table 3.3.

Table 3.3 Phase composition and crystallite size of supports in catalyst preparation

| Chemical | Symbol | %Phase composition (%) | | Crystallite size (nm) |
|--|--------|------------------------|--------|-----------------------|
| | | Anatase | Rutile | |
| P25 | P25 | 87 | 13 | 25 |
| Titanium(IV) oxide, rutile nanopowder, <100 nm particle size, 99.5% trace metals basis | R1 | 0 | 100 | 15 |
| Titanium(IV) oxide, rutile powder, <5 μm, ≥99.9% trace metals basis | R2 | 0 | 100 | N/A |
| Titanium(IV) oxide, anatase nanopowder, <25 nm particle size, 99.7% trace metals basis | A1 | 100 | 0 | 15 |
| Titanium(IV) oxide, anatase nanopowder, 99.7% (metals basis) | A2 | 91 | 9 | 34 |

3.2 Catalyst preparation

3.2.1 Preparation of monometallic Ni/TiO₂ catalysts by incipient wetness impregnation method.

The 15 wt%Ni/TiO₂ catalysts were prepared by impregnation method. Nickel(II) nitrate hexahydrate was dissolved in deionized water and dropped into various phase composition and average crystallite sizes of TiO₂ support (P25, rutile(R1), rutile(R2), anatase(A1) and anatase(A2)). The catalysts were dried in room temperature for 6 h and dried in an oven at 110°C overnight in air. Then, the dried catalysts were calcined in air at 500°C for 2 h. Finally, all the catalyst samples were reduced under H₂ flow (25 ml/min) at 500°C for 3 h. Diagram of Ni on TiO₂ catalysts preparation by incipient wetness impregnation method is shown in Figure 3.1.

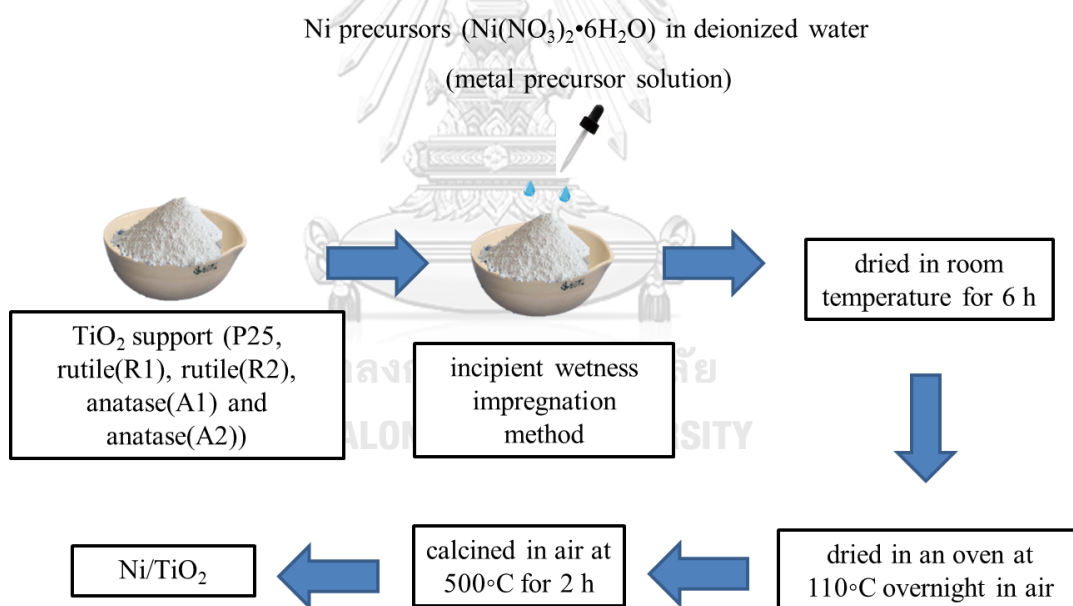


Figure 3.1 Diagram of Ni on TiO₂ catalysts preparation by incipient wetness impregnation method

3.2.2 Preparation of bimetallic Ni-Co/TiO₂ catalysts by incipient wetness co-impregnation method.

The 15 wt% Ni with different amounts of Co (1, 2, 3 wt%) supported on different phase composition and average crystallite sizes of TiO₂ supports were prepared by incipient wetness co-impregnation method. Nickel(II) nitrate hexahydrate and Cobalt(II) nitrate hexahydrate were dissolved in deionized water and dropped into various phase composition and average crystallite sizes of TiO₂ support (P25 and anatase(A2)). The catalysts were dried in room temperature for 6 h and dried in an oven at 110°C overnight in air. Then, the dried catalysts were calcined in air at 500°C for 2 h. Finally, all the catalyst samples were reduced under H₂ flow (25 ml/min) at 500°C for 3 h. Diagram of Ni-Co on TiO₂ catalysts preparation by incipient wetness impregnation method is shown in Figure 3.2.

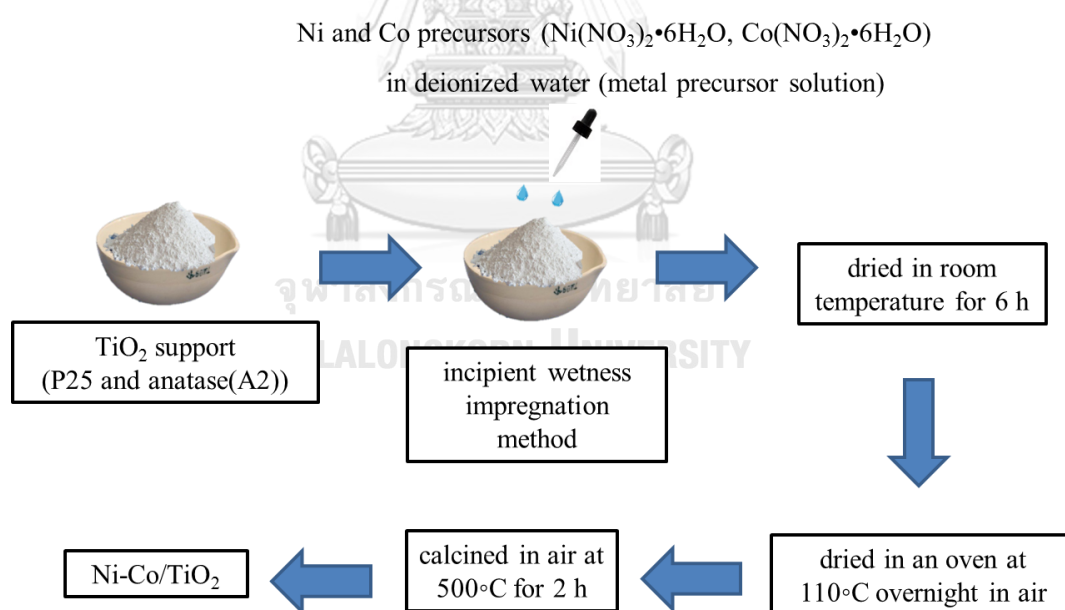


Figure 3.2 Diagram of Ni-Co on TiO₂ catalysts preparation by incipient wetness co-impregnation method

3.3 Catalyst Characterization

3.3.1 X-ray diffraction (XRD)

The X-ray diffraction (XRD) patterns were performed by X-ray diffractometer (Bruker D8 Advance) using Cu K α irradiation in the 2θ range between 20° to 80° with a scan speed 0.5 sec/step. The average crystallite size was calculated using the Scherrer equation.

3.3.2 N₂-physisorption

The BET surface area, average pore size diameters, and average pore volume were measured by using N₂-physisorption in a Micrometrics ASAP 2020 instrument.

3.3.3 Transmission electron spectroscopy (TEM)

Transmission electron spectroscopy (TEM) was used to determine about morphology and crystallite sizes of catalysts by using a JEOL-JEM 2010 transmission electron microscope using energy-dispersive X-ray detector operated at 200 kV.

3.3.4 H₂-Temperature programmed reduction (H₂-TPR)

The reducibility and reduction temperature of catalysts were determined by H₂-temperature programmed reduction (H₂-TPR). The H₂-TPR was carried out in a quartz U-tube reactor using a Micromeritics ChemiSorb 2750 with ChemiSoftTPx software. For TPR profile measurements, all the catalyst samples were pretreated with N₂ gas flow (25 ml/min, 1 h, 150°C). After cooling to 30°C, a gas mixture of 10% H₂ in argon (25 ml/min) was passed through the catalyst samples in quartz U-tube reactor. The temperature was raised from 30°C to 850°C at a heating rate of 10°C /min and held at that temperature for 1 h.

3.3.5 X-ray photoelectron spectroscopy (XPS)

X-ray photoelectron spectra (XPS) of the catalyst samples were performed on the Kratos Amicus x-ray photoelectron spectroscopy. The experiment was operated with the x-ray source at 20 mA and 12 kV (240 W), the resolution at 0.1 eV/step and the pass

energy of the analyzer was set at 75 eV under pressure approximately 1×10^{-6} Pa. For calibration, the binding energy was referenced to C 1s line at 285.0 eV. The binding energy of O 1s, Ni 2p, and Ti 2p are determined.

3.3.6 H₂-pulse chemisorption

The percentages of nickel dispersion and nickel active sites were measured from H₂-pulse chemisorption technique using a Micromeritics ChemiSorb 2750 with ChemiSoftTPx software. Approximately 0.05 g. of catalyst was packed in a quartz U-tube cell and pretreated with helium gas flow (25 ml/min) to exhaust air. Then, the catalyst was reduced under H₂ gas flow (25 ml/min) at 500°C for 3 h with a heating rate of 10°C/min. After catalyst already was reduced, it was cooled down to the room temperature with helium gas. Finally, H₂ gas was injected into the sample cell by pulse method for adsorbing on active sites of catalyst, while unabsorbed H₂ was detected by TCD signal. The injection was stopped when the unabsorbed H₂ peaks were similar height.

3.4 Catalyst test in the furfural hydrogenation

The catalytic performances of sample catalysts were tested in the liquid phase selective hydrogenation of furfural to FA in a 100 mL stainless steel autoclave reactor (JASCO, Tokyo, Japan). Prior to the reaction, sample catalysts were reduced in a flow of H₂ (25 ml/min) at 500°C for 3 h and transferred to the reactor. In a typical reaction, 0.05 g of catalyst, 50 µL of furfural, and 10 mL of methanol were placed in the reactor. The reactor was heated to 50°C and then purged with H₂ to remove the air for three times. After purging, the reactor was pressurized with 20 bar of H₂. The reaction was operated at 50°C, 20 bar of H₂ for 2 h with a stirring speed of 900 rpm. After the reaction, the reactor was cooled to below room temperature with ice water and carefully depressurized. Then, the product solutions were centrifuged to separate the liquid products from the catalyst particles. Finally, the reactant and liquid product samples

were analyzed by a gas chromatograph equipped with a flame ionization detector. Schematic of the liquid-phase hydrogenation of furfural, chemicals used in the liquid-phase furfural hydrogenation, and the operating conditions of gas chromatograph with a flame ionization detector were shown in Figure 3.3, Table 3.4 and Table 3.5, respectively.

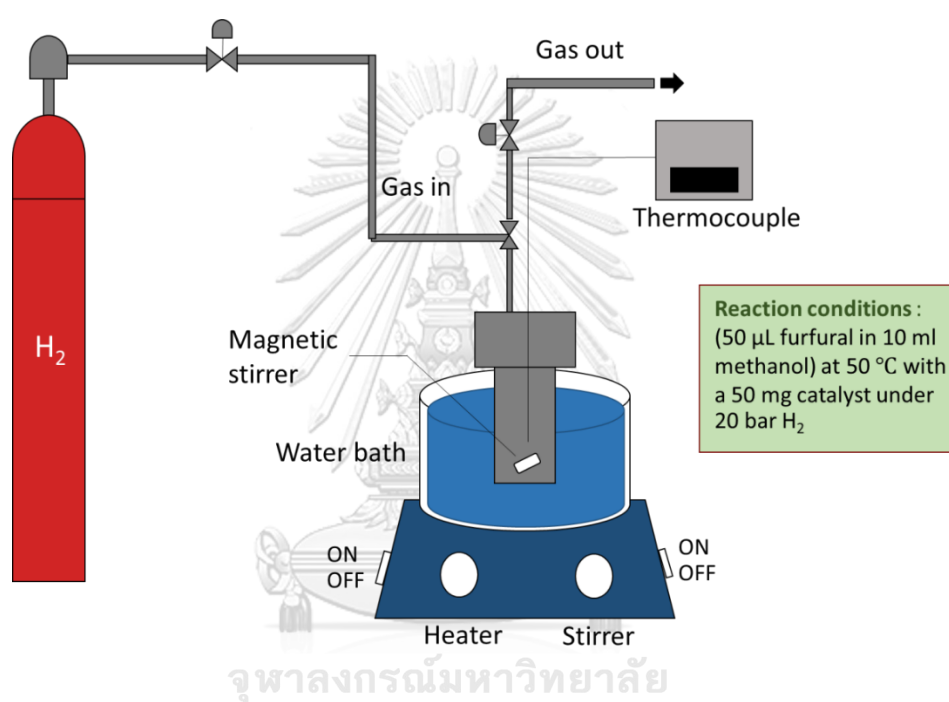


Figure 3.3 Schematic of the liquid-phase hydrogenation of furfural

Table 3.4 Chemicals used in the liquid-phase furfural hydrogenation

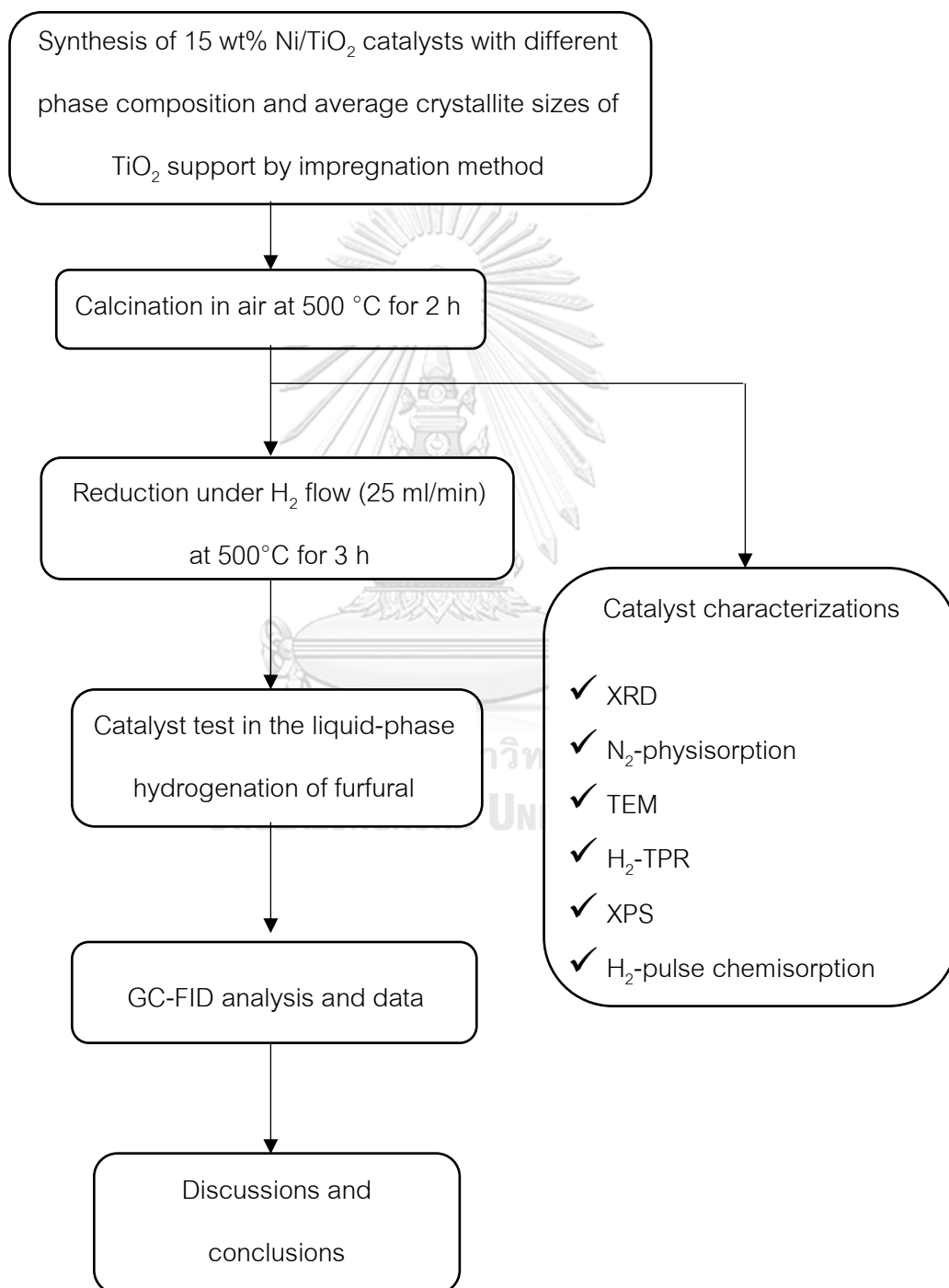
| Chemicals | Formula | Suppliers |
|--------------------------------|----------------|----------------------|
| Furfural 99% | $C_5H_4O_2$ | Aldrich Chemical Ltd |
| Furfuryl alcohol 99% | $C_5H_6O_2$ | Aldrich Chemical Ltd |
| Tetrahydrofurfuryl alcohol 98% | $C_5H_{10}O_2$ | Aldrich Chemical Ltd |
| Methanol 98% | CH_3OH | Aldrich Chemical Ltd |

Table 3.5 The operating conditions of gas chromatograph with a flame ionization detector

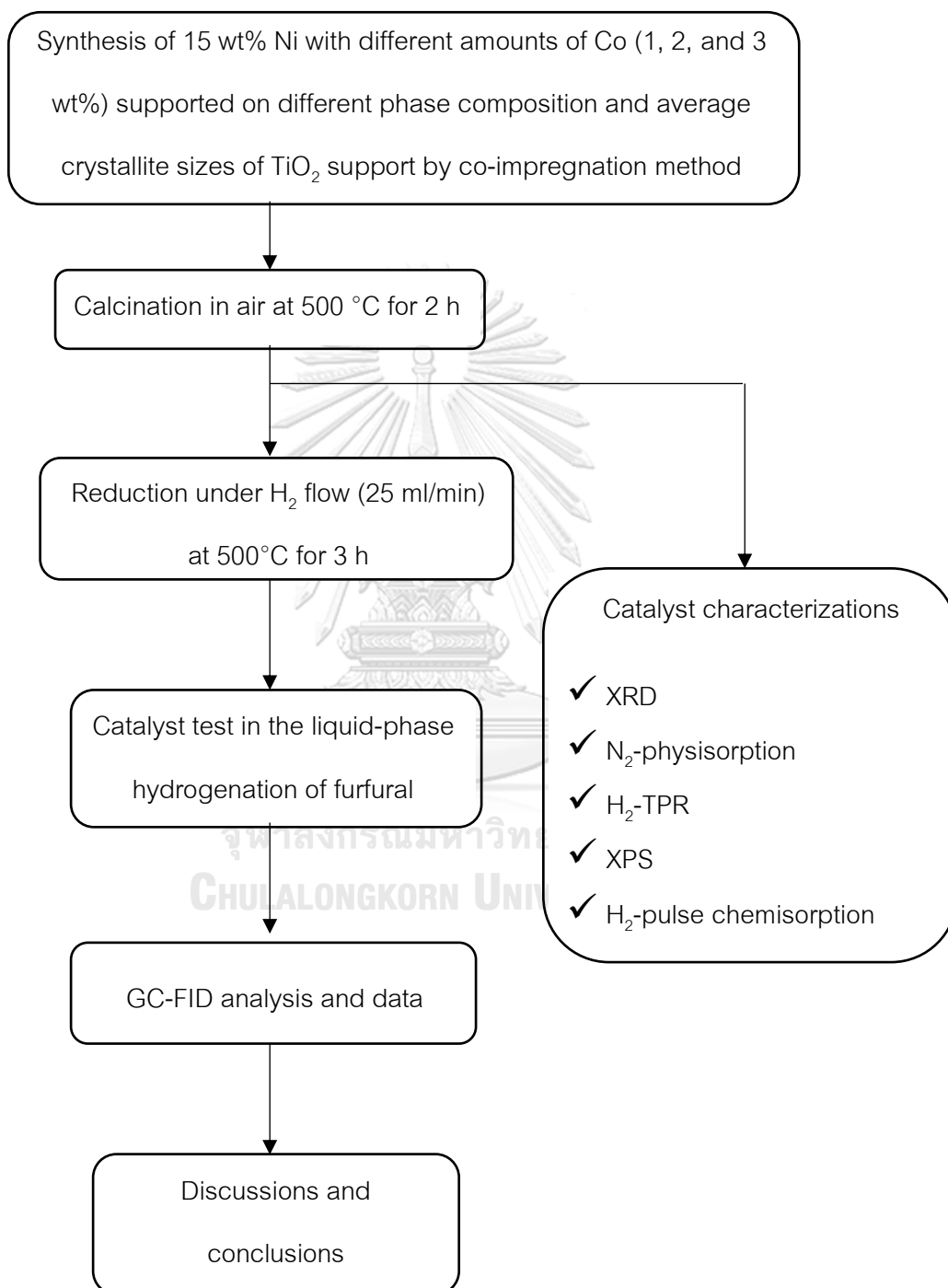
| Gas chromatography (Shimadzu GC-2014) | Conditions |
|---------------------------------------|----------------------|
| Detector | FID |
| Packed column | Rtx®5 |
| Carrier gas | Helium (99.99 vol.%) |
| Make-up gas | Air (99.9 vol.%) |
| Column temperature | 110 °C |
| Injector temperature | 260 °C |
| Detector temperature | 270 °C |
| Time analysis | 41.80 min |

3.5 Research methodology

Part I. The investigation of the characteristics and catalytic performances of Ni nanoparticles supported on different phase composition and average crystallite sizes of TiO₂ support in the liquid-phase furfural hydrogenation



Part II. Study of the effect of bimetallic Ni-Co nanoparticles supported on different phase composition and average crystallite sizes of TiO₂ support in liquid-phase furfural hydrogenation



CHAPTER IV

RESULTS AND DISCUSSION

This chapter explains the detail about the physiochemical and catalytic properties of monometallic Ni/TiO₂ and bimetallic Ni-Co/TiO₂ catalysts that were prepared by impregnation method and co-impregnation method, respectively. The results and discussion is divided into two parts. In the first part, the effects of TiO₂ support on the physiochemical and catalytic properties of monometallic Ni/TiO₂ in the selective hydrogenation of furfural to furfuryl alcohol were investigated. And in the second part, the effect of Co addition on the physiochemical and catalytic properties of bimetallic Ni-Co/TiO₂ catalysts in the selective hydrogenation of furfural to furfuryl alcohol were studied and compared with the monometallic catalysts in the first part. The characterization of the catalyst samples were analyzed by X-ray diffraction (XRD), N₂-physisorption, H₂-temperature programmed reduction (H₂-TPR), X-ray photoelectron spectroscopy (XPS), H₂-pulse chemisorption, Transmission electron spectroscopy (TEM).

Part I. The investigation of the characteristics and catalytic performances of Ni nanoparticles supported on different phase compositions and average crystallite sizes of TiO₂ support in the liquid-phase furfural hydrogenation

4.1 Characterization of Ni/TiO₂ with different phase compositions and average crystallite sizes of TiO₂ support

4.1.1 X-ray diffraction (XRD)

The XRD patterns of the Ni/TiO₂ catalysts with different phase compositions and average crystallite sizes are shown in **Figure 4.1**. The diffraction angles (2θ) were measured from 20° to 80°. The XRD characteristic peaks exhibited anatase phase at $2\theta = 25^\circ$ (major), 37°, 48°, 55°, 56°, 62°, 71°, 75° and rutile phase at 27° (major), 36°, 42°, and 57°[30]. The diffraction peaks of NiO species at $2\theta = 37.3^\circ$, 43.3°, and 62.8° [31]. The average crystallite sizes of TiO₂ supports and NiO species were calculated using the Scherrer's equation from the full width at half maximum of the XRD peak at $2\theta = 25^\circ$ (major) of anatase phase, $2\theta = 27^\circ$ (major) of rutile phase, and $2\theta = 43.3^\circ$ (major) of NiO phase. The amount of anatase phase (% anatase phase) was calculated using the areas of the major anatase at $2\theta = 25^\circ$ and rutile $2\theta = 27^\circ$ of XRD peaks following the method described by Jung et al[32]. The results are summarized in **Table 4.1**. From **Table 4.1**, The NiO particle sizes in Ni/TiO₂-P25, Ni/TiO₂-A1, Ni/TiO₂-A2, Ni/TiO₂-R1, and Ni/TiO₂-R2 catalysts were 12, 10, 12, 12, and 15 nm, respectively.

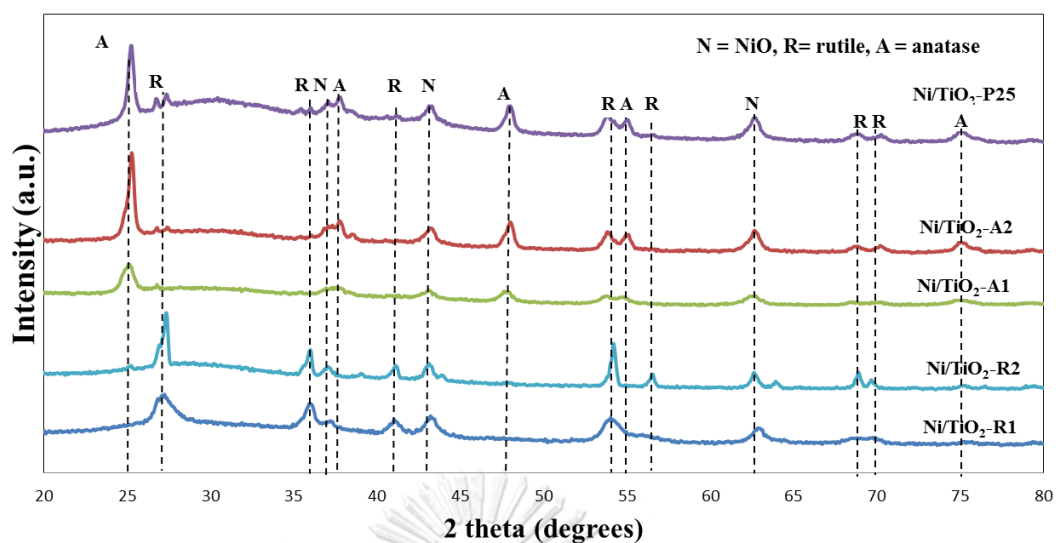


Figure 4.1 The XRD patterns of Ni/TiO₂ catalysts with different phase compositions and average crystallite sizes.

Table 4.1 The average crystallite sizes and %phase composition of the Ni/TiO₂ catalysts with different phase compositions and average crystallite sizes

| Catalyst | Average Crystallite size of TiO ₂ ^a (nm) | Average Crystallite size of NiO ^a (nm) | | %Phase composition ^a | |
|--------------------------|--|---|--------|---------------------------------|--------|
| | | By XRD | By TEM | Anatase | Rutile |
| Ni/TiO ₂ -P25 | 24 ^b | 12 ^d | 13.3 | 93 | 7 |
| Ni/TiO ₂ -A1 | 11 ^b | 10 ^d | 5.6 | 95 | 5 |
| Ni/TiO ₂ -A2 | 25 ^b | 12 ^d | 9.1 | 97 | 3 |
| Ni/TiO ₂ -R1 | 14 ^c | 12 ^d | 7.1 | 0 | 100 |
| Ni/TiO ₂ -R2 | N/A | 15 ^d | 27.8 | 0 | 100 |

^a Based on the XRD results.

^b Determined from anatase peak at 25°

^c Determined from anatase peak at 27°

^d Determined from rutile peak at 43.3°

4.1.2 N₂ Physisorption

The physical properties, such as the BET surface area, average pore size diameters, average pore volume of the Ni/TiO₂ catalysts with different phase compositions and average crystallite sizes were measured by the Brunauer Emmett Teller (BET) method. The results are summarized in **Table 4.2**. From the results, there were no significant differences in BET surface area and average pore volume of Ni/TiO₂-A1, Ni/TiO₂-A2, and Ni/TiO₂-P25, but the average pore size diameter of Ni/TiO₂-A2 was higher than Ni/TiO₂-A1 and Ni/TiO₂-P25. The Ni/TiO₂-A2 showed the highest average pore size at 31.9 nm. However, the Ni/TiO₂-R1 had the highest BET surface area at 93.5 m²/g and the largest average pore volume at 0.568 cm³/g, which corresponded with the N₂ adsorption-desorption isotherms.

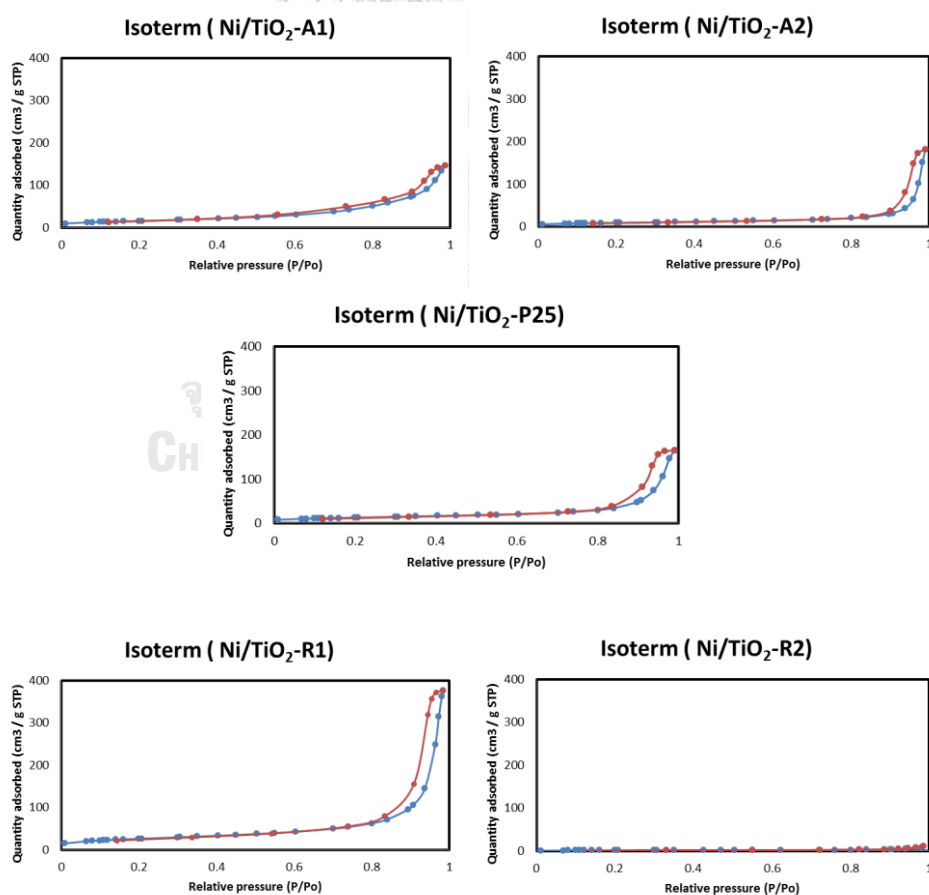


Figure 4.2 N₂-physorption isotherms of Ni/TiO₂-P25, Ni/TiO₂-A1, Ni/TiO₂-A2, Ni/TiO₂-R1, and Ni/TiO₂-R2

The N_2 adsorption-desorption isotherms of Ni/TiO₂-P25, Ni/TiO₂-A1, Ni/TiO₂-A2, Ni/TiO₂-R1, and Ni/TiO₂-R2 are shown in Figure 4.2 and the combination of N_2 adsorption-desorption isotherms of all catalysts are displayed in Figure 4.3. From the results, All the Ni/TiO₂ catalysts with different phase composition and average crystallite sizes exhibited type IV physisorption isotherm that corresponded to the characteristic of mesoporous materials with pore diameters between 2 and 50 nm and the shape characteristic of hysteresis loop for all the catalysts showed type H3 hysteresis loop which referred to the slit shaped pores.

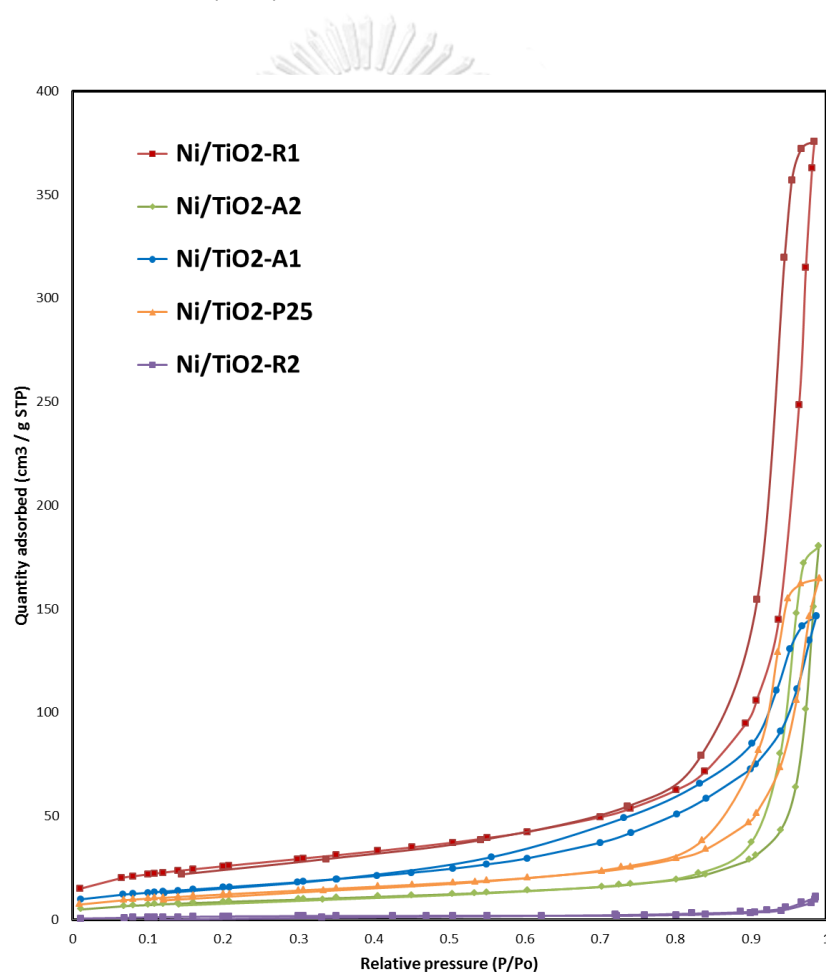


Figure 4.3 The combination of N_2 -physisorption isotherms of Ni/TiO₂-P25, Ni/TiO₂-A1, Ni/TiO₂-A2, Ni/TiO₂-R1, and Ni/TiO₂-R2

Table 4.2 The physical properties of the Ni/TiO₂ catalysts with different phase compositions and average crystallite sizes

| Catalyst | BET surface areas (m ² /g) | Average pore size diameter ^a (nm) | Average pore volume ^a (cm ³ (STP)/g) |
|--------------------------|---------------------------------------|--|--|
| Ni/TiO ₂ -P25 | 44.5 | 22.7 | 0.25 |
| Ni/TiO ₂ -A1 | 56.7 | 15.7 | 0.22 |
| Ni/TiO ₂ -A2 | 31.4 | 31.9 | 0.25 |
| Ni/TiO ₂ -R1 | 93.5 | 24.3 | 0.57 |
| Ni/TiO ₂ -R2 | 6.6 | 8.3 | 0.01 |

^aDetermined from the Barret-Joyner-Halenda (BJH) desorption method.

4.1.3 H₂-temperature programmed reduction (H₂-TPR)

H₂-TPR technique was studied to determine the reducibility, reduction behaviors of Ni/TiO₂ catalysts with different phase compositions and average crystallite sizes, as well as to obtain the information about the interaction between the metal and support. The reduction behaviors of Ni/TiO₂-R1, Ni/TiO₂-R2, Ni/TiO₂-A1, Ni/TiO₂-A2, and Ni/TiO₂-P25 catalysts are shown in **Figure 4.4**. All the Ni/TiO₂ showed two main reduction peaks; except Ni/TiO₂-R2 had one main reduction peaks. The first reduction peak at 300°C - 400°C was a result of the reduction of the bulk NiO oxides in the interaction with TiO₂ support and the second reduction peak at 400°C - 600°C was a result of the reduction of the complex NiO species, which had stronger interaction with TiO₂ support to form NiO-TiO₂ interaction species [33]. From the results, the second reduction peak of NiO on Ni/TiO₂-P25 and Ni/TiO₂-A2 showed larger peak area than other catalysts at 476°C and 462°C, respectively, indicating the presence of a large amount of NiO species that had stronger interaction with TiO₂ support. However, the second reduction peak of NiO on Ni/TiO₂-R1 was the largest at 535°C, which indicated that the oxidation degree of Ni

supported on rutile titania is comparatively higher than anatase titania, so the reduction of nickel oxide to metallic nickel for anatase titania support is easier [17]. Therefore, the variation in the reduction temperature of nickel on different phases of titania could be due to the different intensity of interaction between the metal and the support [20].

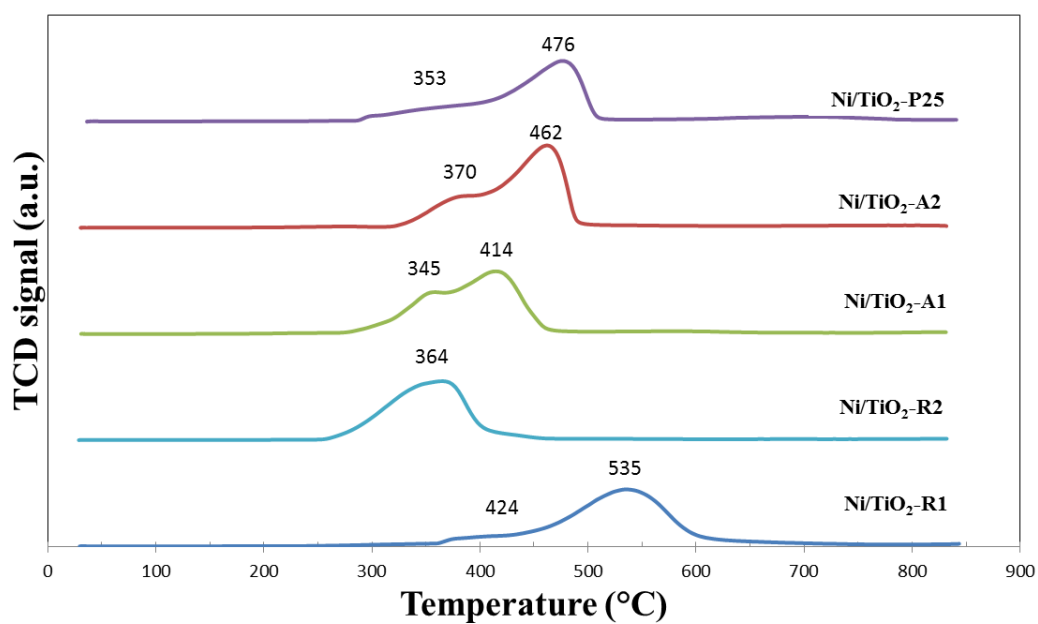


Figure 4.4 H₂-TPR profiles of Ni/TiO₂ catalysts with different phase compositions and average crystallite sizes

4.1.4 Transmission electron spectroscopy (TEM)

TEM technique was studied to determine the morphology and metal particles size of Ni/TiO₂ catalysts with different phase compositions and average crystallite sizes are shown in Figure 4.5. The average particle size of NiO on Ni/TiO₂-A1, Ni/TiO₂-A2, Ni/TiO₂-P25, Ni/TiO₂-R1, and Ni/TiO₂-R2 catalysts determined from the TEM images were approximately as 5.6, 9.1, 13.3, 7.1, 27.8 nm, respectively. From TEM results, it was found that Ni/TiO₂-A1 and Ni/TiO₂-R1 had much smaller size of NiO particles, while Ni/TiO₂-R2 had fairly large size. The NiO particle size on Ni/TiO₂-P25 and Ni/TiO₂-A2 were in between these two sets of catalysts. The TEM results correspond well with the results of XRD and XPS.

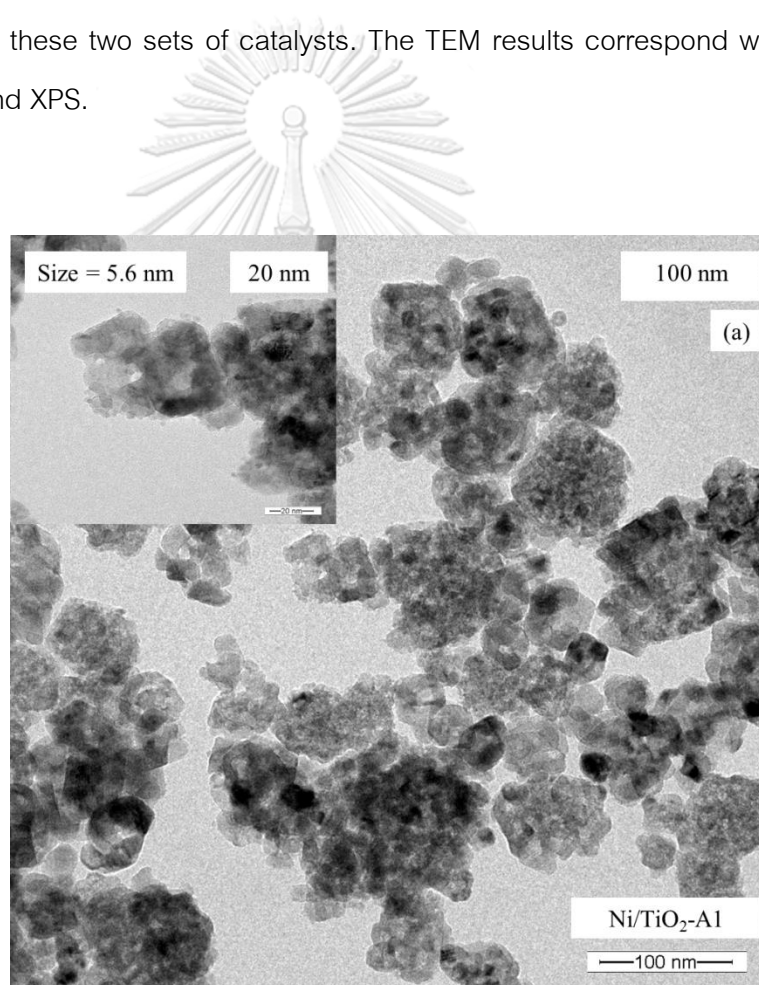


Figure 4.5 TEM images of the Ni/TiO₂ catalysts: (a) Ni/TiO₂-A1; (b) Ni/TiO₂-A2; (c) Ni/TiO₂-P25; (d) Ni/TiO₂-R1; and (e) Ni/TiO₂-R2

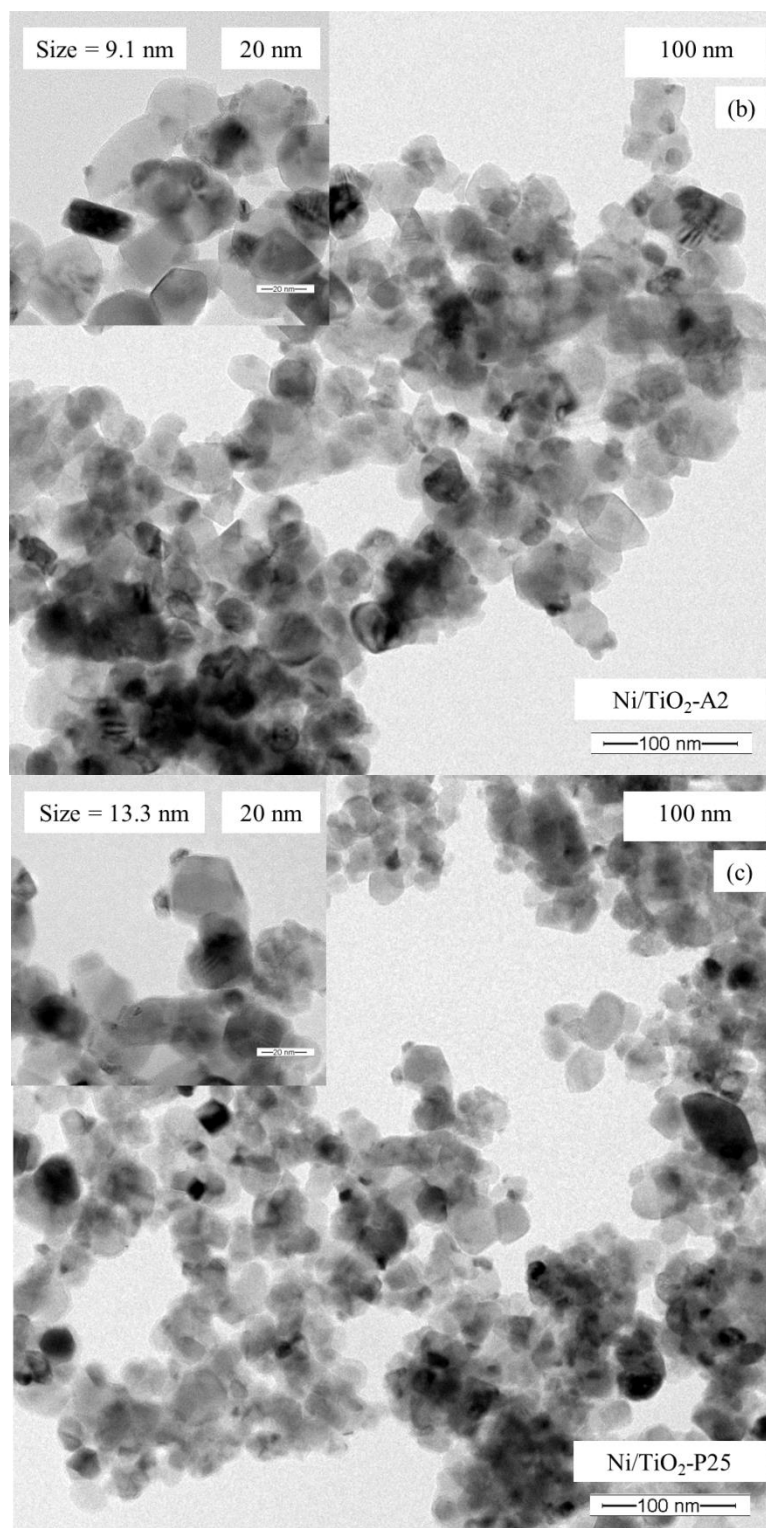


Figure 4.5 TEM images of the Ni/TiO₂ catalysts: (a) Ni/TiO₂-A1; (b) Ni/TiO₂-A2; (c) Ni/TiO₂-P25; (d) Ni/TiO₂-R1; and (e) Ni/TiO₂-R2

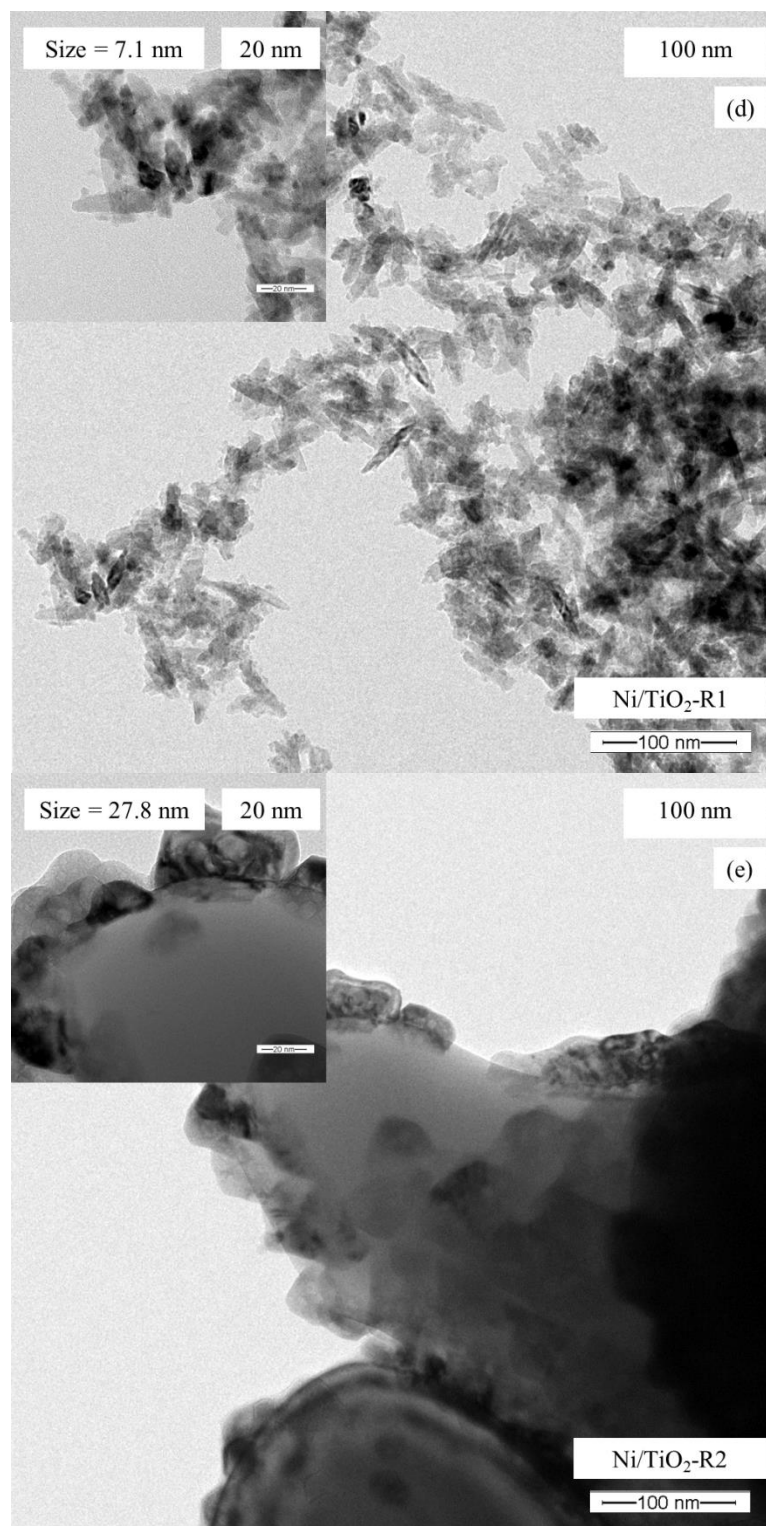


Figure 4.5 TEM images of the Ni/TiO₂ catalysts: (a) Ni/TiO₂-A1; (b) Ni/TiO₂-A2; (c) Ni/TiO₂-P25; (d) Ni/TiO₂-R1; and (e) Ni/TiO₂-R2

4.1.5 X-ray photoelectron spectroscopy (XPS)

The elemental composition of the catalyst at surface and electronic states were investigated by X-ray photoelectron spectroscopy (XPS). The XPS results are shown in **Figure 4.6**. In principle, the Ni2p_{3/2} spectra for NiO exhibited a characteristic doublet structure (855.4 eV and 853.8 eV) with a peak width (FWHM) of 4.7 eV and a satellite located at 860.7 eV [34]. From the XPS results, a main peak at 853.8 eV and 855.4 eV could be observed for Ni/TiO₂-P25, Ni/TiO₂-A1, and Ni/TiO₂-A2, which is consistent with the reported Ni2p_{3/2} binding energy, indicating the presence of discrete NiO and highly dispersed NiO species, respectively. For Ni/TiO₂-R1 and Ni/TiO₂-R2, the Ni2p_{3/2} spectra exhibited only a main peak at 855.4 eV and 853.8 eV, respectively. In addition, the surface atomic composition of the Ni/TiO₂ catalysts with different phase composition and average crystallite sizes are shown in **Table 4.3**. From the results, it was found that Ni/TiO₂-P25, Ni/TiO₂-A2, and Ni/TiO₂-A1 had relatively high atomic ratios of Ni/Ti (0.6-1). Whilst the Ni/TiO₂-R2 and Ni/TiO₂-R1 had the highest (3.2) and lowest (0.3) atomic ratios of Ni/Ti, respectively. All above results accorded with the H₂-TPR analysis and TEM images.

Table 4.3 The surface atomic composition of the Ni/TiO₂ catalysts with different phase compositions and average crystallite sizes

| Catalyst | Atomic concentration | | | Atomic ratio |
|--------------------------|----------------------|--------|-------|--------------|
| | Ni (%) | Ti (%) | O (%) | Ni/Ti |
| Ni/TiO ₂ -P25 | 16.9 | 15.5 | 67.6 | 1.094 |
| Ni/TiO ₂ -A1 | 15.3 | 15.6 | 69.1 | 0.984 |
| Ni/TiO ₂ -A2 | 7.3 | 11.9 | 80.8 | 0.619 |
| Ni/TiO ₂ -R1 | 4.2 | 13.7 | 82.1 | 0.306 |
| Ni/TiO ₂ -R2 | 22.3 | 7.1 | 70.6 | 3.166 |

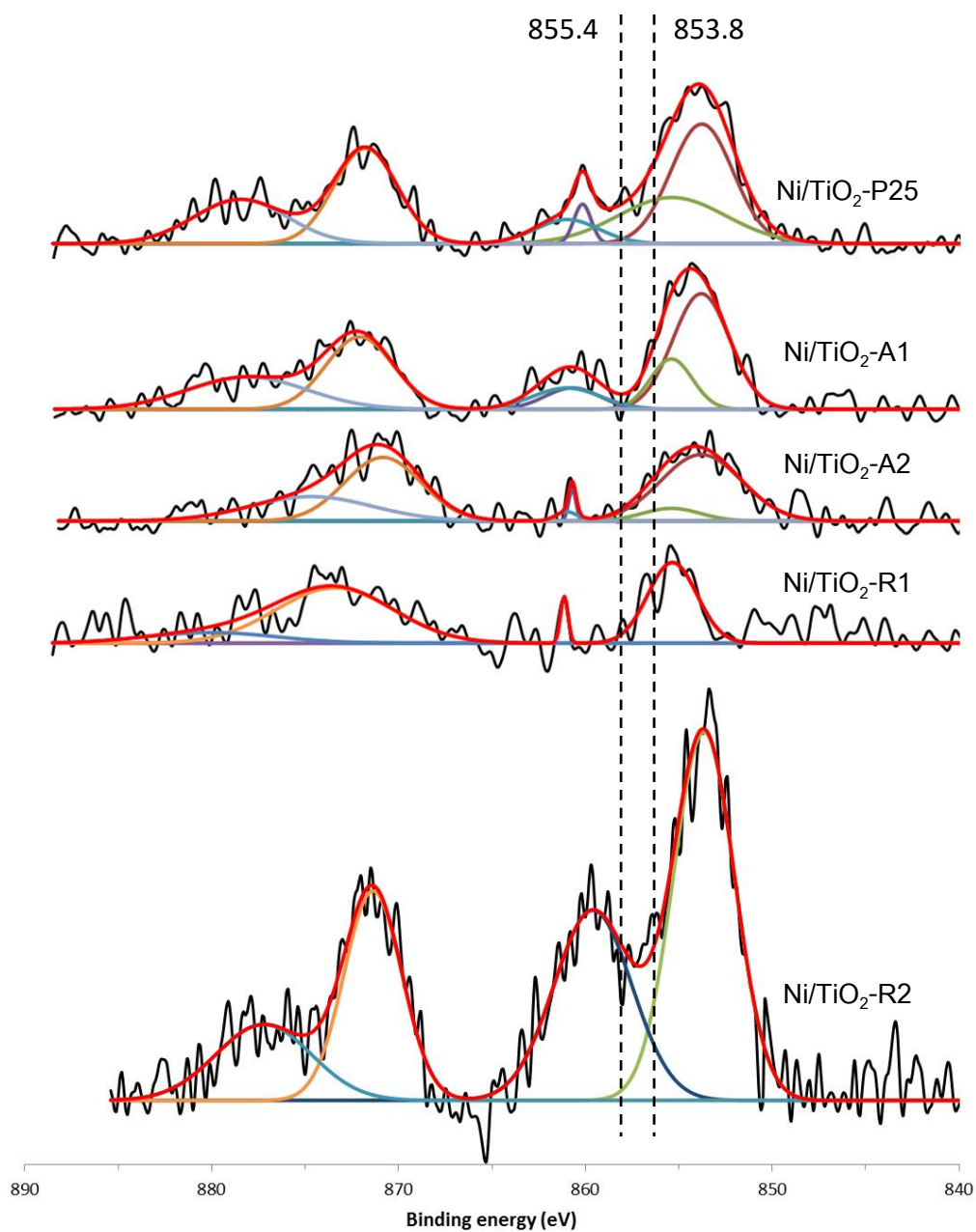


Figure 4.6 Ni 2p peak in XPS spectra of Ni/TiO₂ with catalysts with different phase compositions and average crystallite sizes

4.1.6 H₂-pulse Chemisorption (H₂-chem)

The amounts of Ni active sites and %Ni dispersion on Ni/TiO₂ catalysts with different phase compositions and average crystallite sizes were determined by the chemisorption based on the assumption H : Ni = 2 : 1. All catalysts were reduced under H₂ flow at 500°C before H₂ injection to adsorb on active sites. The results are shown in **Table 4.4**. From the results, the %Ni dispersion on Ni/TiO₂-A1, Ni/TiO₂-A2, Ni/TiO₂-P25, Ni/TiO₂-R1, and Ni/TiO₂-R2 catalysts showed at 0.056%, 0.077%, 1.561%, 0.008%, and 0%, respectively. It was found that Ni dispersion on Ni/TiO₂-A1 and Ni/TiO₂-A2 were similar and higher than Ni/TiO₂-R1, and Ni/TiO₂-R2. Moreover, the dispersion of Ni on TiO₂-R2 was the lowest and Ni on TiO₂-P25 was the highest that corresponded well with the N₂-physisorption results as shown in **Table 4.2**. Considering %Ni dispersion, it was found that the dispersion of Ni on TiO₂ support was affected by phase composition of TiO₂. As observed from **Table 4.1**, the catalysts that had high anatase phase were also had high dispersion of Ni owing to anatase phase of TiO₂ are favorable adsorption sites for hydrogen atoms than rutile phase [35]. Therefore, these catalysts had more Ni active sites for interaction with hydrogen atoms that resulted in increased %Ni dispersion.

Table 4.4 The H₂ chemisorption and metal concentrations of the Ni/TiO₂ catalysts with different phase compositions and average crystallite sizes

| Catalyst | Ni actual loading ^a (%wt) | Amount of active sites (x10 ¹⁸) (x10 ¹⁸ molecule H ₂ /g cat) | %Ni dispersion ^b |
|--------------------------|---|--|-----------------------------|
| Ni/TiO ₂ -P25 | 13.6 | 21.76 | 1.561 |
| Ni/TiO ₂ -A1 | 12.9 | 0.74 | 0.056 |
| Ni/TiO ₂ -A2 | 14.0 | 1.11 | 0.077 |
| Ni/TiO ₂ -R1 | 15.1 | 0.13 | 0.008 |
| Ni/TiO ₂ -R2 | 12.4 | 0 | 0 |

^a Results from inductively coupled plasma (ICP)

^b Determined from H₂-pulse chemisorption technique with the chemisorption based on the assumption H : Ni = 2 : 1

4.2 Activity test in the liquid-phase furfural hydrogenation

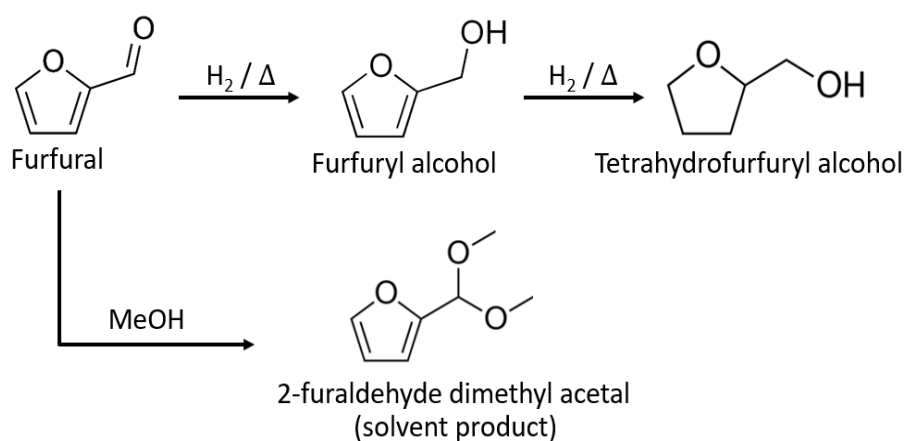


Figure 4.7 The pathways of furfural hydrogenation reaction [22]

The pathways of furfural hydrogenation reaction are shown in **Figure 4.7**. From the **Figure 4.7** It exhibited the 2 main reaction pathways. The first pathway is the hydrogenation in 2 steps of the C=O bond that transformed furfural to furfuryl alcohol and then furfuryl alcohol is hydrogenated at the C=C bond to produce tetrahydrofurfuryl alcohol. However, when using some organic solvent, the side reaction product between furfural and solvent may be occurred. In this study, the second pathway occurred due to hydrogenation of C=O bond with methanol, which converted furfural to 2-furaldehyde dimethyl acetal (solvent product, labeled as SP) [22]. Furfuryl alcohol (FA) is the desired product and tetrahydrofurfuryl alcohol (THFA) and 2-furaldehyde dimethyl acetal (SP) are the undesired products.

The catalytic performances of Ni/TiO₂ catalysts with different phase compositions and average crystallite sizes were investigated in the selective hydrogenation of furfural to furfuryl alcohol (FA) under the following reaction conditions: 50°C, 20 bars of H₂ and 2 h reaction time by using methanol as the solvent. The reaction results of the catalytic behaviors of the Ni/TiO₂ with different phases composition and average crystallite sizes including furfural conversion and product selectivity are reported in **Table 4.5**. It was found that the Ni/TiO₂-A2 catalyst exhibited the highest furfural activity under the reaction conditions with the highest furfural yield under the reaction conditions. The superior catalytic performances of the Ni/TiO₂-A2 could be attributed to the dispersion of Ni on support and interaction between metal and support as shown in **Table 4.4** and **Figure 4.4**, respectively. The catalytic activity decreased with the decreasing of the interaction between metal and support. This result suggested that the interaction between metal and support was the important factor attributing to the catalytic activity of Ni catalyst in the selective hydrogenation of furfural to furfuryl alcohol (FA). From **Figure 4.4**, the H₂ consumption that indicating about the strong interaction between metal and

support of Ni/TiO₂-P25, Ni/TiO₂-A2, and Ni/TiO₂-R1 were quite similar, so catalytic activity of these catalysts showed rather similar and higher than Ni/TiO₂-A1 and Ni/TiO₂-R2.

However, the selectivity of furfuryl alcohol was correlated more with the dispersion of Ni. Dispersion of Ni was another important factor affecting to the selectivity of furfuryl alcohol. From **Table 4.4**, Ni/TiO₂-P25, Ni/TiO₂-A1, and Ni/TiO₂-A2 had higher dispersion of Ni than Ni/TiO₂-R1 and Ni/TiO₂-R2 catalyst due to anatase phase of TiO₂ are favorable adsorption sites for hydrogen atoms. In contrast, rutile phase TiO₂ could not be interacted strongly with molecular hydrogen, while atomic hydrogen readily sticks to the surface oxygen atoms [35]. Therefore, the main factors to improve the catalytic activity and selectivity of furfuryl alcohol were the strong interaction between metal and support and good dispersion of Ni on the support.

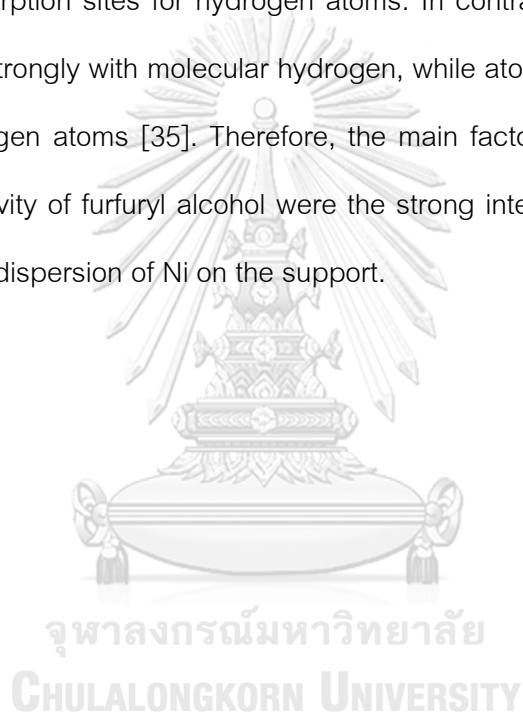


Table 4.5 The catalytic performances of Ni/TiO₂ catalysts with different phase compositions and average crystallite sizes

| Entry | Catalyst | Conversion (%) | Selectivity (%) | | | | FA Yield (%) |
|-------|--------------------------|----------------|-----------------|-------------------|-----------------|-------|--------------|
| | | | FA ^a | THFA ^b | SP ^c | Other | |
| 1 | Ni/TiO ₂ -P25 | 79.33 | 50.81 | 18.42 | - | 30.77 | 40.31 |
| 2 | Ni/TiO ₂ -A1 | 4.73 | 76.52 | - | 23.48 | - | 3.62 |
| 3 | Ni/TiO ₂ -A2 | 65.69 | 66.74 | 9.71 | 1.49 | 22.06 | 43.84 |
| 4 | Ni/TiO ₂ -R1 | 71.5 | 49.75 | 13.81 | 1.07 | 35.37 | 35.57 |
| 5 | Ni/TiO ₂ -R2 | 26.97 | 60.11 | 8.78 | 8.22 | 22.89 | 16.21 |

Reaction (50 μ L furfural in 10 ml methanol) at 50°C under 20 bar H₂ with a 50 mg catalyst in 2 hours

^a Selectivity of furfuryl alcohol (FA)

^b Selectivity of tetrahydrofurfuryl alcohol (THFA)

^c Selectivity of 2-furaldehyde dimethyl acetal (SP)

Part II. Study of the effect of bimetallic Ni-Co nanoparticles supported on anatase (A2) and P25 phase of TiO₂ catalyst in the selective hydrogenation of furfural to furfuryl alcohol.

4.3 Characterization of Ni-Co/TiO₂ with different Co contents

4.3.1 X-ray diffraction (XRD)

In Figure 4.8 showed the XRD patterns of Ni/TiO₂-A2 and Ni-Co/TiO₂-A2 catalysts with different Co contents that were varied at 1, 2, and 3%wt with 15%wt of Ni on TiO₂-A2. The catalysts were prepared by the incipient wetness co-impregnation method. The XRD patterns were measured at the diffraction angles (2θ) between 20° to 80°. Both monometallic and bimetallic catalysts exhibited the characteristic of anatase phase at $2\theta = 25^\circ$ (major), 37°, 48°, 55°, 56°, 62°, 71°, 75° and rutile phase at 27° (major), 36°, 42°, and 57° [30]. In addition, these catalysts showed the characteristic of NiO species at $2\theta = 37.3^\circ$, 43.3°, and 62.8° [31]. The peaks corresponding to Co were not detected probably due to low amount of metal present and/or high dispersion of metal on the TiO₂ supports [13].

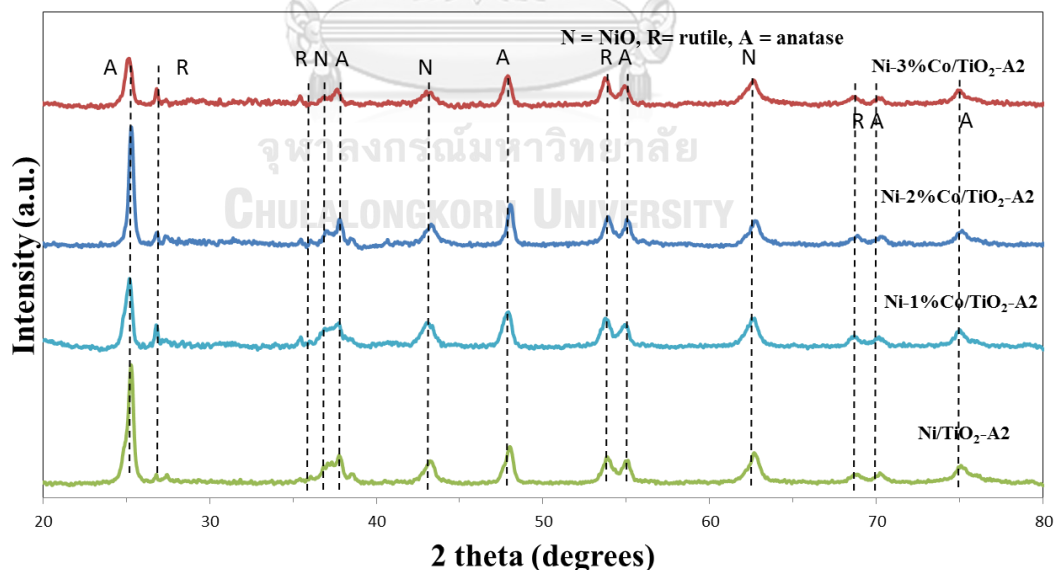


Figure 4.8 The XRD patterns of Ni/TiO₂-A2 and Ni-Co/TiO₂-A2 catalysts with different Co contents

The average crystallite sizes of anatase phase TiO₂ supports and NiO species were calculated using the Scherrer's equation from the full width at half maximum of the XRD peak at $2\theta = 25^\circ$ (major) of anatase phase, and $2\theta = 43.3^\circ$ (major) of NiO phase, respectively. The average crystallite size of TiO₂ supports, NiO particle, and the amount of %anatase phase of the TiO₂ support of synthesis catalysts are performed in Table 4.6. From Table 4.6, The NiO particle sizes in all catalysts were approximately 10-13 nm. Moreover, it found that %anatase phase was decrease, when Co was added. This observation suggest that it could be occur from the formation of Co new phase. However, this phase could not be detected in the XRD results due to low amount of Co addition.

Table 4.6 The average crystallite sizes and %phase composition of the Ni/TiO₂-A2 and Ni-Co/TiO₂ catalysts with different Co contents

| Catalyst | Average Crystallite size of TiO ₂ ^a (nm) | Average Crystallite size of NiO ^a (nm) | %Phase composition ^{a,b} | |
|-------------------------------|--|---|-----------------------------------|--------|
| | | By XRD | Anatase | Rutile |
| Ni/TiO ₂ -A2 | 25 | 12 | 97 | 3 |
| Ni-1%Co/TiO ₂ -A2 | 18 | 10 | 90 | 10 |
| Ni-2%Co/TiO ₂ -A2 | 32 | 11 | 93 | 7 |
| Ni-3%Co/TiO ₂ -A2 | 18 | 12 | 88 | 12 |
| Ni-2%Co/TiO ₂ -P25 | 18 | 13 | 82 | 18 |

^a Based on the XRD results.

^b Determined from Jung et al. method.

4.3.2 N₂ Physisorption

The BET surface area, average pore size diameters, average pore volume of the Ni/TiO₂-A2 and Ni-Co/TiO₂ catalysts were measured by the Brunauer Emmett Teller (BET) method as shown in Table 4.7. From the results, BET surface area, average pore volume, and average pore diameter were no significant differences at around 31 to 35 m²/g, 0.22 to 0.25 cm³/g and 24 to 32 nm, respectively. Thus, Co adding slightly affected BET surface area, average pore volume, and average pore diameter.

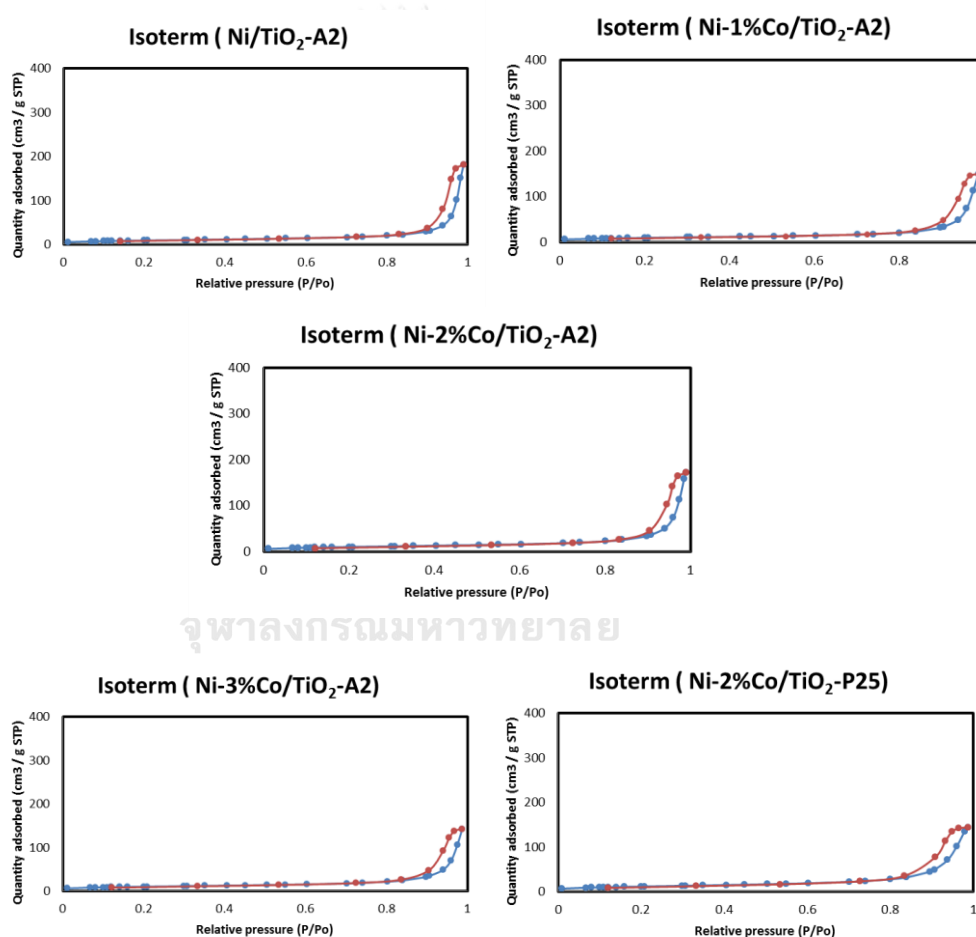


Figure 4.9 The N₂-physorption isotherms of Ni/TiO₂-A2, Ni-1%Co/TiO₂-A2, Ni-2%Co/TiO₂-A2, Ni-3%Co/TiO₂-A2, and Ni-2%Co/TiO₂-P25

The N_2 adsorption-desorption isotherms of Ni/TiO₂-A2 and Ni-Co/TiO₂ catalysts are shown in Figure 4.9 and the combination of N_2 adsorption-desorption isotherms of all catalysts are displayed in Figure 4.10. From the results, Both the Ni/TiO₂-A2 and Ni-Co/TiO₂ catalysts exhibited type IV physisorption isotherm, which indicating about the characteristic of mesoporous materials with pore diameters between 2 and 50 nm. In addition, the shape characteristic of hysteresis loop for all the catalysts showed type H3 hysteresis loop which corresponded to the slit shaped pores and/or panel-shaped particles.

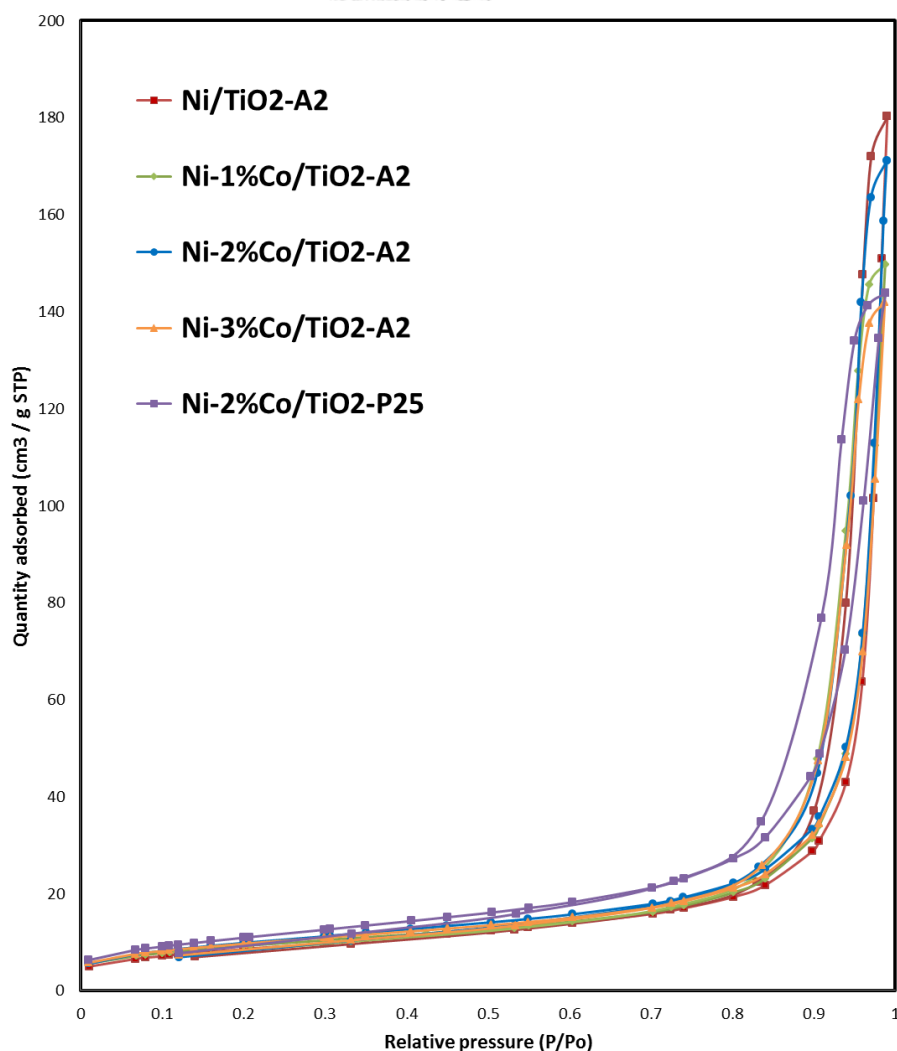


Figure 4.10 Combination of N_2 -physisorption isotherms of Ni/TiO₂-A2 and Ni-Co/TiO₂ catalysts

Table 4.7 The physical properties of the Ni/TiO₂-A2 and Ni-Co/TiO₂ catalysts with different Co contents

| Catalyst | BET surface areas (m ² /g) | Average pore size diameter ^a (nm) | Average pore volume ^a (cm ³ (STP)/g) |
|-------------------------------|---------------------------------------|--|--|
| Ni/TiO ₂ -A2 | 31.4 | 31.9 | 0.25 |
| Ni-1%Co/TiO ₂ -A2 | 33.5 | 27.2 | 0.23 |
| Ni-2%Co/TiO ₂ -A2 | 34.2 | 27.6 | 0.25 |
| Ni-3%Co/TiO ₂ -A2 | 35.1 | 24.7 | 0.22 |
| Ni-2%Co/TiO ₂ -P25 | 39.8 | 22.1 | 0.22 |

^a Determined from the Barret-Joyner-Halenda (BJH) desorption method.

4.3.3 H₂-temperature programmed reduction

The reduction behaviors of the monometallic Ni/TiO₂-A2 and bimetallic Ni-Co/TiO₂-A2 catalysts with different Co contents were studied by H₂-TPR technique. The results are performed in **Figure 4.11**. Both monometallic and bimetallic catalysts showed two main reduction peaks. The first reduction peak at 300°C - 400°C correlated to the reduction of the bulk NiO oxides in the interaction with TiO₂ support and the second reduction peak at 400°C - 600°C indicated to the reduction of the complex NiO species, which had stronger interaction with TiO₂ support to form NiO-TiO₂ interaction species. [33]. According to the results, Co addition into Ni based catalyst slightly modified the H₂-TPR profiles of the catalysts. The first reduction peaks of all catalysts were similar, but the second reduction peaks were shifted to lower reduction temperatures when Co addition increased, suggesting weaker interaction between metal and TiO₂ support. It is possibly due to simultaneous reduction and/or alloy formation [11]. In addition, the reduction peaks of cobalt oxides were not detected in the TPR profiles of Ni-Co/TiO₂-A2 [36], suggesting low amount of Co loading as also confirmed by XRD results in **Figure 4.8**.

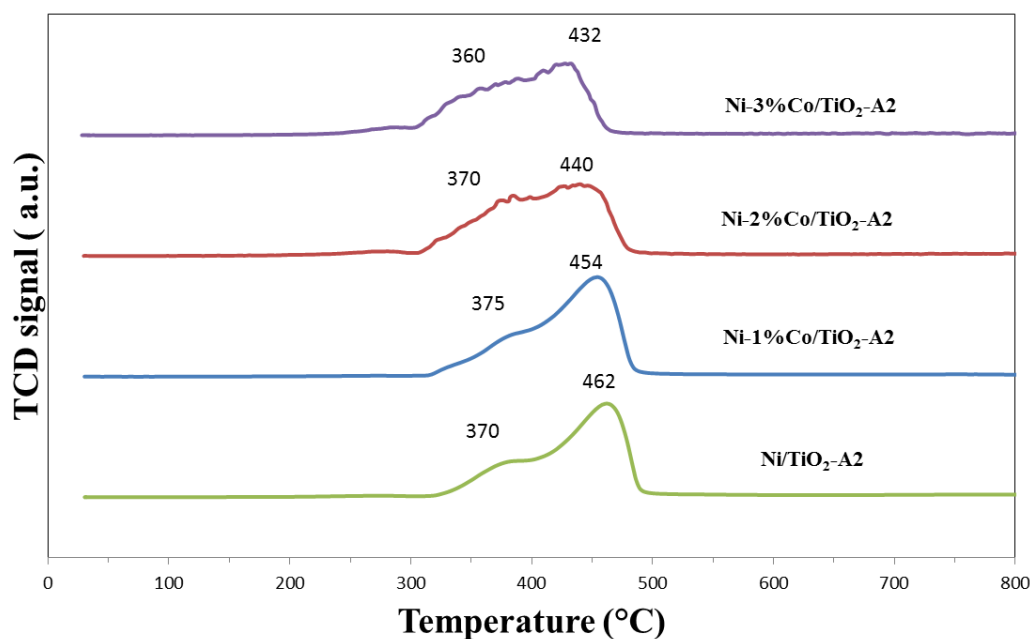


Figure 4.11 The H₂-TPR profiles of Ni/TiO₂-A2 and Ni-Co/TiO₂-A2 catalysts with different Co contents

4.3.4 X-ray photoelectron spectroscopy (XPS)

The X-ray photoelectron spectroscopy (XPS) technique was applied to determine the elemental composition and electronic states of the synthetic catalyst at surface. The XPS results are shown in Figure 4.12. All of the binding energies in the XPS analysis were corrected for specimen charging by referencing them to the C 1s peak (285 eV). From XPS results, binding energy value at 853.8 eV and 855.4 eV could be observed for Ni2p_{3/2} energy level in monometallic Ni/TiO₂ catalysts, which indicating to discrete NiO and highly dispersed NiO species, respectively [34]. Bimetallic Ni-Co/TiO₂-A2 catalysts showed a shifting of the binding energy of Ni2p_{3/2} peak. The binding energy of Ni2p_{3/2} was shifted to higher binding energy when compared with monometallic Ni/TiO₂-A2 catalysts. The shift in binding energy might be due to the partial electronic transfer between Ni and Co in the formation of alloys. [37].

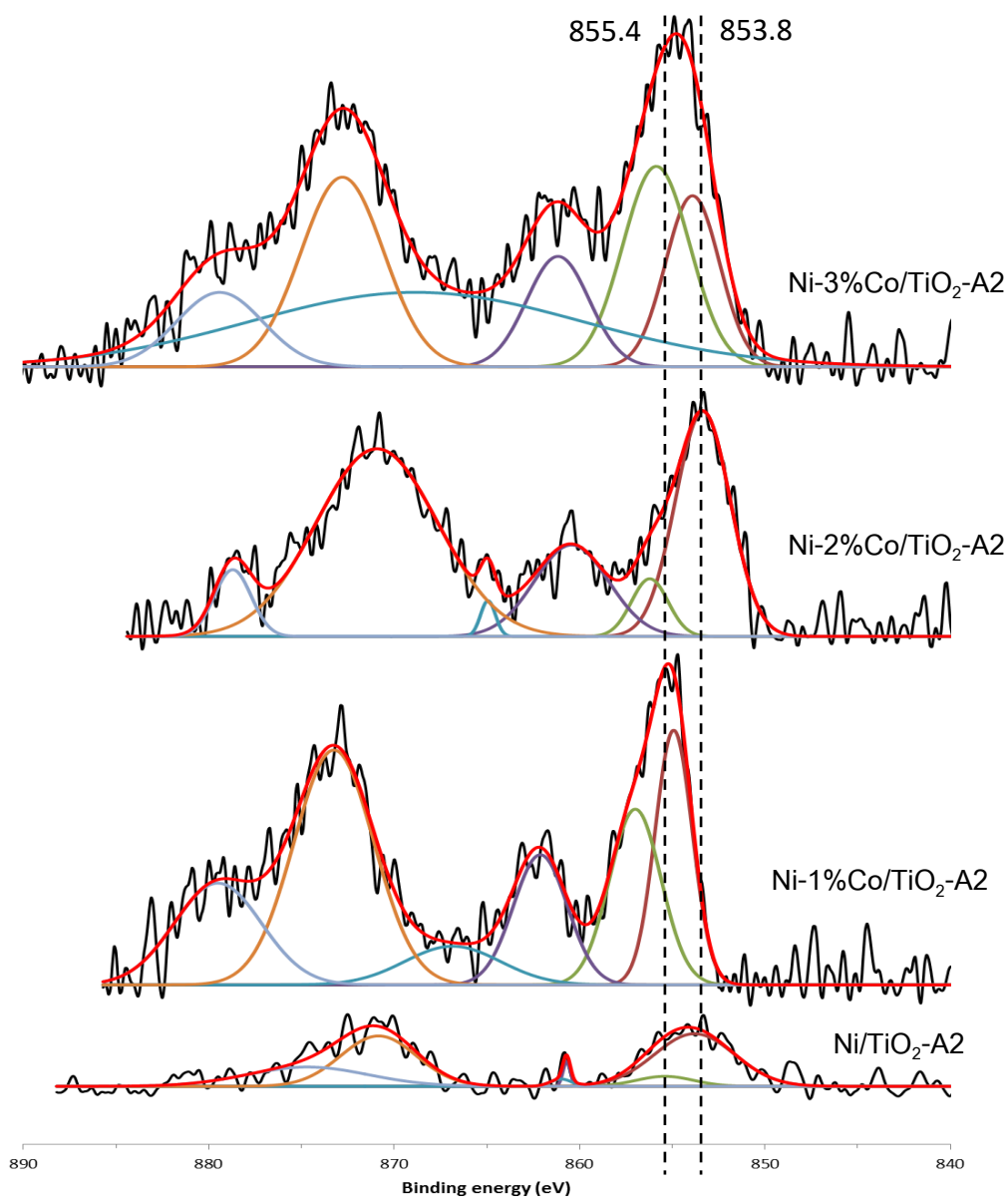


Figure 4.12 Ni 2p peak in XPS spectra of Ni/TiO₂-A2 and Ni-Co/TiO₂-A2 catalysts with different Co contents

4.3.5 H₂-pulse Chemisorption (H₂-chem)

The amounts of active Ni sites and %Ni dispersion on Ni/TiO₂-A2 and Ni-Co/TiO₂ catalysts with different Co contents were measured by the H₂chemisorption, which based on the assumption H:Ni = 2:1. All catalysts were reduced under H₂ flow at 500°C before H₂ injection to adsorb on active sites. It can be observed from **Table 4.8**. From the results, the Ni/TiO₂-A2, Ni-1%Co/TiO₂-A2, Ni-2%Co/TiO₂-A2, and Ni-3%Co/TiO₂-A2 catalysts showed the Ni dispersion at 0.077%, 0.337%, 0.942%, and 0.119%, respectively. Considering Co addition, it was found that the increasing amount of Co loading on Ni/TiO₂ catalysts resulted in increased %Ni dispersion. As observed from H₂-TPR results, the reducibility of the catalysts increased with increasing in Co loading until the amount of Co loading was 2%, so more active sites were available for H₂ chemisorption that resulted in increased %Ni dispersion [38]. However, Co addition exceeding 2%wt caused decreasing of %Ni dispersion.

Table 4.8 The H₂ chemisorption and metal concentrations of the Ni/TiO₂-A2 and Ni-Co/TiO₂ catalysts with different Co contents

| Catalyst | Amount of active sites (x10 ¹⁸) (x10 ¹⁸ molecule H ₂ /g cat) | %Ni dispersion ^{a,b} |
|-------------------------------|--|-------------------------------|
| Ni/TiO ₂ -A2 | 1.11 | 0.077 |
| Ni-1%Co/TiO ₂ -A2 | 5.18 | 0.337 |
| Ni-2%Co/TiO ₂ -A2 | 14.49 | 0.942 |
| Ni-3%Co/TiO ₂ -A2 | 1.83 | 0.119 |
| Ni-2%Co/TiO ₂ -P25 | 4.08 | 0.265 |

^a Results from 15% of Ni

^b Determined from H₂-pulse chemisorption technique with the chemisorption based on the assumption H : Ni = 2 : 1

4.4 The catalytic performances of Ni/TiO₂ and Ni-Co/TiO₂ catalysts with different Co content in the liquid-phase furfural hydrogenation

The catalytic behaviors of the monometallic Ni/TiO₂-A2 and bimetallic Ni-Co/TiO₂-A2 catalysts with different Co contents at 1, 2, and 3%wt including furfural conversion and selectivity of furfuryl alcohol are summarized in **Table 4.9**. From **Table 4.9**, the monometallic Ni/TiO₂ catalyst showed furfural conversion and FA selectivity at 65.69% and 66.74%, respectively. For bimetallic catalyst, Co addition into monometallic Ni/TiO₂ catalyst affected to decreased furfural conversion with little change on the FA selectivity. According to the XPS results, the addition of Co into Ni/TiO₂ catalyst affected to the peak of Ni2p_{3/2} by shifting to higher binding energy, which suggested the partial electronic transfer between Ni and Co in the formation of alloys [37]. From H₂-TPR results, the second reduction peaks were shifted to lower temperature reduction suggesting a weaker interaction between metal and TiO₂ support. As observed from H₂-chemisorption results, the %Ni dispersion was increased when Co was added to Ni/TiO₂ catalyst. It might be suggested that %Ni dispersion was correlated with the reducibility of the catalysts [38], corresponding to both XPS and H₂-TPR results.

In addition, the catalytic behaviors of the monometallic Ni/TiO₂-P25 and bimetallic Ni-Co/TiO₂-P25 catalysts with Co contents at 2%wt including furfural conversion and selectivity of furfuryl alcohol are summarized in **Table 4.10**. From **Table 4.10**, it was found that all of results in **Table 4.10** had the same trend with the results in **Table 4.9**.

From these reasons, the addition of Co into Ni/TiO₂ catalysts on P25 and A2 TiO₂ supports made the furfural conversion decreased with a slight change on the FA selectivity when compared to the monometallic Ni/TiO₂. This result was happened possibly due to simultaneous reduction and/or alloy formation [11].

In the comparison between Ni-2%Co/TiO₂-A2 and Ni-2%Co/TiO₂-P25, it was found that Ni-2%Co/TiO₂-P25 showed a lower yield of furfuryl alcohol than Ni-2%Co/TiO₂-A2 despite its higher furfural conversion. This result may be depending on other factors, such as the kinds of metal and the physical properties of supports.

Table 4.9 The catalytic performances of Ni/TiO₂-A2 and Ni-Co/TiO₂-A2 catalysts with different Co contents

| Catalyst | Conversion (%) | Selectivity (%) | | | | FA Yield (%) |
|------------------------------|----------------|-----------------|-------------------|-----------------|-------|--------------|
| | | FA ^a | THFA ^b | SP ^c | Other | |
| Ni/TiO ₂ -A2 | 65.69 | 66.74 | 9.71 | 1.49 | 22.06 | 43.84 |
| Ni-1%Co/TiO ₂ -A2 | 46.47 | 70.19 | 6.75 | 2.32 | 20.74 | 32.62 |
| Ni-2%Co/TiO ₂ -A2 | 53.71 | 71.62 | 7.94 | 0.76 | 19.68 | 38.47 |
| Ni-3%Co/TiO ₂ -A2 | 14.66 | 85 | 0 | 7.16 | 7.84 | 12.46 |

Reaction (50 μ L furfural in 10 ml methanol) at 50°C under 20 bar H₂ with a 50 mg catalyst in 2 hours

^a Selectivity of furfuryl alcohol (FA)

^b Selectivity of tetrahydrofurfuryl alcohol (THFA)

^c Selectivity of 2-furaldehyde dimethyl acetal (SP)

Table 4.10 The catalytic performances of Ni/TiO₂-P25 and Ni-2%Co/TiO₂-P25 catalysts

| Catalyst | Conversion (%) | Selectivity (%) | | | | FA Yield (%) |
|-------------------------------|----------------|-----------------|-------------------|-----------------|-------|--------------|
| | | FA ^a | THFA ^b | SP ^c | Other | |
| Ni/TiO ₂ -P25 | 79.33 | 50.81 | 18.42 | - | 30.77 | 40.31 |
| Ni-2%Co/TiO ₂ -P25 | 65.97 | 44.08 | 24.37 | 2.89 | 28.66 | 29.08 |

Reaction (50 μ L furfural in 10 ml methanol) at 50°C under 20 bay H₂ with a 50 mg catalyst in 2 hours

^a Selectivity of furfuryl alcohol (FA)

^b Selectivity of tetrahydrofurfuryl alcohol (THFA)

^c Selectivity of 2-furaldehyde dimethyl acetal (SP)

CHAPTER V

CONCLUSIONS

5.1 Conclusions

From the first part, dispersion of Ni on support and interaction between metal and support of Ni/TiO₂ catalysts with different phase composition and average crystallite sizes correlated with the catalytic performances of the catalysts. The catalytic activity decreased with the decreasing of the interaction between metal and support. In contrast, the selectivity of furfuryl alcohol was rather affected by the dispersion of Ni. Among the catalysts studied, the Ni/TiO₂-A2 catalyst exhibited the best performances with the furfural conversion, selectivity of furfuryl alcohol, and furfural yield under the reaction conditions used at 65.7%, 66.7%, and 43.84%, respectively.

In the second part, Co addition to the monometallic Ni/TiO₂ catalysts, simultaneous reduction and/or alloy formation may occur corresponding to the XPS and H₂-TPR results, resulting in lower reduction temperature of the NiO and/or weaker –Ni-TiO₂ interaction. As a consequence, the bimetallic catalysts exhibited poorer catalyst performances compared to the monometallic Ni/TiO₂, regardless of the nature of the TiO₂ used.

5.2 Recommendation

1. The interaction between Ni and Co should be investigated by more sophisticated techniques.
2. The other product in hydrogenation of furfural that does not know should be researched.
3. The reusability of the synthesized catalysts should be investigated.

REFERENCES

- [1]. Jia, P.; Lan, X.; Li, X.; Wang, T., Highly Active and Selective NiFe/SiO₂ Bimetallic Catalyst with Optimized Solvent Effect for the Liquid-Phase Hydrogenation of Furfural to Furfuryl Alcohol. *ACS Sustainable Chemistry & Engineering* **2018**, 6 (10), 13287-13295.
- [2]. Kotbagi, T. V.; Gurav, H. R.; Nagpure, A. S.; Chilukuri, S. V.; Bakker, M. G., Highly efficient nitrogen-doped hierarchically porous carbon supported Ni nanoparticles for the selective hydrogenation of furfural to furfuryl alcohol. *RSC Advances* **2016**, 6 (72), 67662-67668.
- [3]. Bhogeswararao, S.; Srinivas, D., Catalytic conversion of furfural to industrial chemicals over supported Pt and Pd catalysts. *Journal of Catalysis* **2015**, 327, 65-77.
- [4]. Zhang, C.; Lai, Q.; Holles, J. H., Bimetallic overlayer catalysts with high selectivity and reactivity for furfural hydrogenation. *Catalysis Communications* **2017**, 89, 77-80.
- [5]. Rodiansono; Astuti, M. D.; Mujiyanti, D. R.; Santoso, U. T.; Shimazu, S., Novel preparation method of bimetallic Ni-In alloy catalysts supported on amorphous alumina for the highly selective hydrogenation of furfural. *Molecular Catalysis* **2018**, 445, 52-60.
- [6]. Mandalika, A.; Qin, L.; Sato, T. K.; Runge, T., Integrated biorefinery model based on production of furans using open-ended high yield processes. *Green Chem.* **2014**, 16 (5), 2480-2489.
- [7]. Wu, Q.; Zhang, C.; Zhang, B.; Li, X.; Ying, Z.; Liu, T.; Lin, W.; Yu, Y.; Cheng, H.; Zhao, F., Highly selective Pt/ordered mesoporous TiO₂-SiO₂ catalysts for hydrogenation of cinnamaldehyde: The promoting role of Ti(2.). *J Colloid Interface Sci* **2016**, 463, 75-82.
- [8]. Prashar, A. K.; Mayadevi, S.; Nandini Devi, R., Effect of particle size on selective hydrogenation of cinnamaldehyde by Pt encapsulated in mesoporous silica. *Catalysis Communications* **2012**, 28, 42-46.
- [9]. Yang, X.; Mueanngern, Y.; Baker, Q. A.; Baker, L. R., Crotonaldehyde hydrogenation on platinum–titanium oxide and platinum–cerium oxide catalysts: selective C=O bond hydrogen requires platinum sites beyond the oxide–metal interface. *Catalysis Science & Technology* **2016**, 6 (18), 6824-6835.

- [10]. Prakash, M. G.; Mahalakshmy, R.; Krishnamurthy, K. R.; Viswanathan, B., Studies on Ni–M (M = Cu, Ag, Au) bimetallic catalysts for selective hydrogenation of cinnamaldehyde. *Catalysis Today* **2016**, *263*, 105-111.
- [11]. Ashokkumar, S.; Ganesan, V.; Ramaswamy, K. K.; Balasubramanian, V., Bimetallic Co–Ni/TiO₂ catalysts for selective hydrogenation of cinnamaldehyde. *Research on Chemical Intermediates* **2018**, *44* (11), 6703-6720.
- [12]. Seemala, B.; Cai, C. M.; Kumar, R.; Wyman, C. E.; Christopher, P., Effects of Cu–Ni Bimetallic Catalyst Composition and Support on Activity, Selectivity, and Stability for Furfural Conversion to 2-Methylfuran. *ACS Sustainable Chemistry & Engineering* **2017**, *6* (2), 2152-2161.
- [13]. Liu, R.; Yu, Y.; Yoshida, K.; Li, G.; Jiang, H.; Zhang, M.; Zhao, F.; Fujit, S.-i.; Arai, M., Physically and chemically mixed TiO₂-supported Pd and Au catalysts_ unexpected synergistic effects on selective hydrogenation of citral in supercritical CO₂. *Journal of Catalysis* **269** (1), 191-200.
- [14]. Nickel. <https://en.wikipedia.org/wiki/Nickel>.
- [15]. Physical properties of nickel. <https://www.lookchem.com/Periodic-Table/Nickel/>.
- [16]. Bagheri, S.; Muhd Julkapli, N.; Bee Abd Hamid, S., Titanium dioxide as a catalyst support in heterogeneous catalysis. *ScientificWorldJournal* **2014**, *2014*, 727496.
- [17]. Chen, R.; Du, Y.; Xing, W.; Xu, N., The Effect of Titania Structure on Ni/TiO₂ Catalysts for p-Nitrophenol Hydrogenation. *Chinese Journal of Chemical Engineering* **2006**, *14* (5), 665-669.
- [18]. Jongsomjit, B.; Wongsalee, T.; Prasertdam, P., Characteristics and catalytic properties of Co/TiO₂ for various rutile:anatase ratios. *Catalysis Communications* **2005**, *6* (11), 705-710.
- [19]. Yao, N.; Chen, J.; Zhang, J.; Zhang, J., Influence of support calcination temperature on properties of Ni/TiO₂ for catalytic hydrogenation of o-chloronitrobenzene to o-chloroaniline. *Catalysis Communications* **2008**, *9* (6), 1510-1516.
- [20]. Raj, K. J. A.; Prakash, M. G.; Mahalakshmy, R.; Elangovan, T.; Viswanathan, B., Selective hydrogenation of acetophenone over nickel supported on titania. *Catalysis*

Science & Technology **2012**, *2* (7).

- [21]. O'Driscoll, Á.; Leahy, J. J.; Curtin, T., The influence of metal selection on catalyst activity for the liquid phase hydrogenation of furfural to furfuryl alcohol. *Catalysis Today* **2017**, *279*, 194-201.
- [22]. Taylor, M. J.; Durndell, L. J.; Isaacs, M. A.; Parlett, C. M. A.; Wilson, K.; Lee, A. F.; Kyriakou, G., Highly selective hydrogenation of furfural over supported Pt nanoparticles under mild conditions. *Applied Catalysis B: Environmental* **2016**, *180*, 580-585.
- [23]. Vargas-Hernández, D.; Rubio-Caballero, J. M.; Santamaría-González, J.; Moreno-Tost, R.; Mérida-Robles, J. M.; Pérez-Cruz, M. A.; Jiménez-López, A.; Hernández-Huesca, R.; Maireles-Torres, P., Furfuryl alcohol from furfural hydrogenation over copper supported on SBA-15 silica catalysts. *Journal of Molecular Catalysis A: Chemical* **2014**, *383-384*, 106-113.
- [24]. Musci, J. J.; Merlo, A. B.; Casella, M. L., Aqueous phase hydrogenation of furfural using carbon-supported Ru and RuSn catalysts. *Catalysis Today* **2017**, *296*, 43-50.
- [25]. Liu, L.; Lou, H.; Chen, M., Selective hydrogenation of furfural to tetrahydrofurfuryl alcohol over Ni/CNTs and bimetallic Cu Ni/CNTs catalysts. *International Journal of Hydrogen Energy* **2016**, *41* (33), 14721-14731.
- [26]. Fu, Z.; Wang, Z.; Lin, W.; Song, W.; Li, S., High efficient conversion of furfural to 2-methylfuran over Ni-Cu/Al₂O₃ catalyst with formic acid as a hydrogen donor. *Applied Catalysis A: General* **2017**, *547*, 248-255.
- [27]. Cobalt. <https://en.wikipedia.org/wiki/Cobalt#Applications>.
- [28]. Physical properties of cobalt. <https://www.lookchem.com/Periodic-Table/Cobalt/>.
- [29]. Zheng, R.; Porosoff, M. D.; Weiner, J. L.; Lu, S.; Zhu, Y.; Chen, J. G., Controlling hydrogenation of C=O and C=C bonds in cinnamaldehyde using silica supported Co-Pt and Cu-Pt bimetallic catalysts. *Applied Catalysis A: General* **2012**, *419-420*, 126-132.
- [30]. Mekasuwandumrong, O.; Phothakwanpracha, S.; Jongsomjit, B.; Shotipruk, A.; Panpranot, J., Influence of flame conditions on the dispersion of Pd on the flame spray-derived Pd/TiO₂ nanoparticles. *Powder Technology* **2011**, *210* (3), 328-331.
- [31]. Sang, S.; Wang, Y.; Zhu, W.; Xiao, G., Selective hydrogenation of furfuryl alcohol

to tetrahydrofurfuryl alcohol over Ni/V-Al₂O₃ catalysts. *Research on Chemical Intermediates* **2016**, 43 (2), 1179-1195.

[32]. Ramprakash Upadhyay, P.; Srivastava, V., Selective Hydrogenation of CO to methane over TiO₂-supported Ruthenium nanoparticles. *Materials Today: Proceedings* **2016**, 3 (10), 4093-4096.

[33]. Wu, C.; Wang, L.; Williams, P. T.; Shi, J.; Huang, J., Hydrogen production from biomass gasification with Ni/MCM-41 catalysts: Influence of Ni content. *Applied Catalysis B: Environmental* **2011**, 108-109, 6-13.

[34]. Huo, W.; Zhang, C.; Yuan, H.; Jia, M.; Ning, C.; Tang, Y.; Zhang, Y.; Luo, J.; Wang, Z.; Zhang, W., Vapor-phase selective hydrogenation of maleic anhydride to succinic anhydride over Ni/TiO₂ catalysts. *Journal of Industrial and Engineering Chemistry* **2014**, 20 (6), 4140-4145.

[35]. Islam, M. M.; Calatayud, M.; Pacchioni, G., Hydrogen Adsorption and Diffusion on the Anatase TiO₂(101) Surface: A First-Principles Investigation. *The Journal of Physical Chemistry C* **2011**, 115 (14), 6809-6814.

[36]. YueLiu;; YuejunWang;; HaiqiangWang;; ZhongbiaoWu;, Catalytic oxidation of gas-phase mercury over Co/TiO₂ catalysts prepared by sol-gel method. **2011**, 12 (14), 1291-1294.

[37]. Zada, B.; Yan, L.; Fu, Y., Effective conversion of cellobiose and glucose to sorbitol using non-noble bimetallic NiCo/HZSM-5 catalyst. *Science China Chemistry* **2018**, 61 (9), 1167-1174.

[38]. Zada, B.; Yan, L.; Fu, Y., Carbon monoxide hydrogenation over zirconia supported NiCo/HZSM-5 catalyst. *SCIENCE CHINA Chemistry* **2018**, 61, 1167-1174.

APPENDIX A

CALCULATION FOR CARALYST PREPARATION

The calculation of monometallic 15 wt%Ni/TiO₂ catalysts and bimetallic 15 wt%Ni/TiO₂ catalysts with different amounts of 1-3 wt%Co prepared by incipient wetness impregnation method were shown below.

In this work, the compositions of catalysts were based on 2 g of catalyst used as follows:

Reagents: Nickel(II) nitrate hexahydrate (Ni(NO₃)₂•6H₂O), MW = 290.79 g/mol

Cobalt(II) nitrate hexahydrate (Co(NO₃)₂•6H₂O), MW = 291.03 g/mol

Calculation of the monometallic 15 wt%Ni/TiO₂ catalysts:

Nickel required = (2×15)/100 = 0.3 g

TiO₂ required = 2-0.01 = 1.7 g

Nickel required in precursor = $\frac{\text{MW. of Ni(NO}_3)_2 \cdot 6\text{H}_2\text{O} \times \text{weight of nickel required}}{\text{MW. of nickel}}$

$$= \frac{290.79 \times 0.3}{58.693}$$

= 1.4863 g.

Calculation of the bimetallic 15 wt%Ni/TiO₂ catalysts with 1-3 wt%Co:

For 15 wt%Ni-2wt%Co/TiO₂

Nickel required = (2×15)/100 = 0.3 g

Cobalt required = (2×2)/100 = 0.04 g

TiO₂ required = 2-0.3-0.04 = 1.66 g

$$\text{Nickel required in precursor} = \frac{\text{MW. of Ni(NO}_3)_2 \cdot 6\text{H}_2\text{O} \times \text{weight of cobalt required}}{\text{MW. of cobalt}}$$

$$= \frac{290.79 \times 0.3}{58.693}$$

$$= 1.4863 \text{ g.}$$

$$\text{Cobalt required in precursor} = \frac{\text{MW. of Co(NO}_3)_2 \cdot 6\text{H}_2\text{O} \times \text{weight of nickel required}}{\text{MW. of nickel}}$$

$$= \frac{291.03 \times 0.04}{58.933}$$

$$= 0.1975 \text{ g.}$$

APPENDIX B

CALCULATION OF THE CRYSTALLITE SIZE

Calculation of the crystallite size by Debye-Scherrer equation

The crystallite size calculation from the width at half of height or full width of the diffraction peak of the XRD pattern using the Debye-Scherrer equation.

From Scherrer equation

$$D = \frac{\kappa\lambda}{\beta \cos\theta}$$

Where D= Crystallite size, Å

K = crystallite-shape factor=0.9

λ = X-ray wavelength, 1.5418 Å for CuK α

θ = Observed peak angle, degree

β = X-ray diffraction broadening, radian

X-ray diffraction broadening (β) is the corrected width of a powder diffraction free from all broadening due to the instrument. The α -alumina was used as a standard sample to observe the instrumental broadening data. The most common correction for the X-ray diffraction broadening (β) can be obtained by

From Warren's formula:

$$\beta = \sqrt{B_m^2 - B_s^2}$$

Where B_M = The measured peak width in radians at half peak height

B_s = The corresponding width of the standard material

APPENDIX C

CALCULATION OF THE PHASE COMPOSITION

The fraction of crystal phase of TiO_2 was determined from X-ray diffraction. The phase composition of TiO_2 was calculated from:

$$W_R = \frac{1}{0.884 \times \frac{A}{R} + 1} \times 100$$

Where W_R = the percentage of rutile

A = the peak area of anatase TiO_2 at (101)

R = the peak area of rutile TiO_2 at (101)

The number of 0.884 is the coefficient of scattering

APPENDIX D

CALCULATION FOR METAL ACTIVE SITES AND DISPERSION

Calculation of Ni active sites and Ni dispersion of the catalyst by H₂-chemisorption is as follows:

$$\text{Volume of CO adsorption on catalyst, } V_{\text{ads}} = \frac{V_{\text{inj}}}{m} \times \sum_{i=1}^n \left(1 - \frac{A_i}{A_r} \right)$$

Where V_{inj} = volume injected, 0.01 cm³

m = mass of catalyst used, g

A_i = area of peak i

A_r = area of last peak

Ni active sites

$$\text{Ni active site} = S_f \times \frac{V_{\text{ads}}}{V_g} \times N_A$$

Where S_f = stoichiometry factor, H₂ adsorbed on Ni, H: Ni = 2: 1

V_{ads} = volume adsorbed

V_g = molar volume of gas at STP, 22414 cm³/mol

N_A = Avogadro's number, 6.023x10²³ molecules/mol

Metal dispersion

$$\text{Metal dispersion (\%)} = 100 \times \frac{\text{molecule of Ni loaded}}{\text{molecule of Ni from H}_2 \text{ adsorption}}$$

$$\%D = S_f \times \frac{V_{\text{ads}}}{V_g} \times \frac{\text{MW}}{\%M} \times 100\% \times 100\%$$

Where S_f = stoichiometry factor, H_2 adsorbed on Ni, H: Ni = 2: 1

V_{ads} = volume adsorbed

V_g = molar volume of gas at STP, $22414 \text{ cm}^3/\text{mol}$

MW = molecular weight of the metal

$\%M$ = weight percent of the active metal

APPENDIX E

CALCULATION FOR CATALYTIC PERFORMANCE

The catalysts performances for the furfural hydrogenation are shown in this below.

$$\% \text{Conversion} = \frac{\text{Mole (in)} - \text{Mole (out)}}{\text{Mole (in)}} \times 100$$

$$\% \text{Selectivity} = \frac{\text{Mole of product}}{\text{Mole of convert reactant}} \times 100$$

$$\% \text{Yield} = \text{conversion} \times \text{selectivity}$$

Example:

$$\% \text{Furfural conversion} = \frac{\text{Mole of furfural (in)} - \text{Mole of furfural (out)}}{\text{Mole of furfural (in)}} \times 100$$

$$\% \text{Furfuryl alcohol selectivity} = \frac{\text{Mole of furfuryl alcohol}}{\text{Mole of converted furfural}} \times 100$$

$$\% \text{ Furfuryl alcohol Yield} = \text{Furfural conversion} \times \text{Furfuryl alcohol selectivity}$$

The calibration curves of furfural, furfuryl alcohol, and tetrahydrofurfuryl alcohol are shown in Figure E1, Figure E2, and Figure E3, respectively.

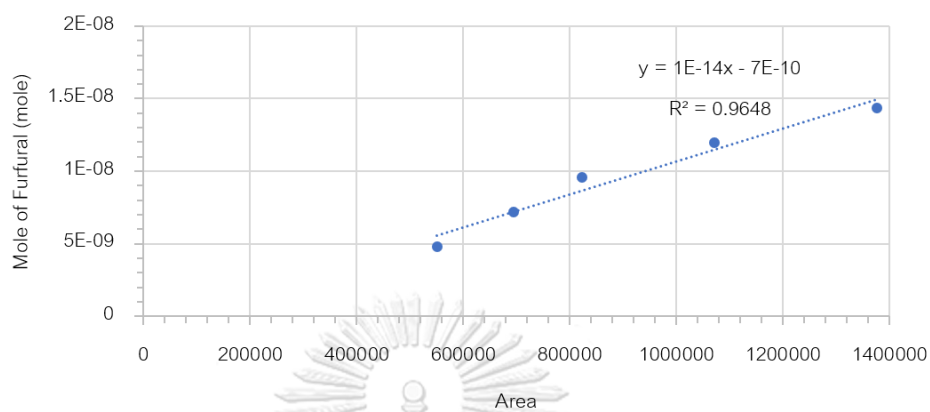


Figure E.1 The calibration curve of furfural

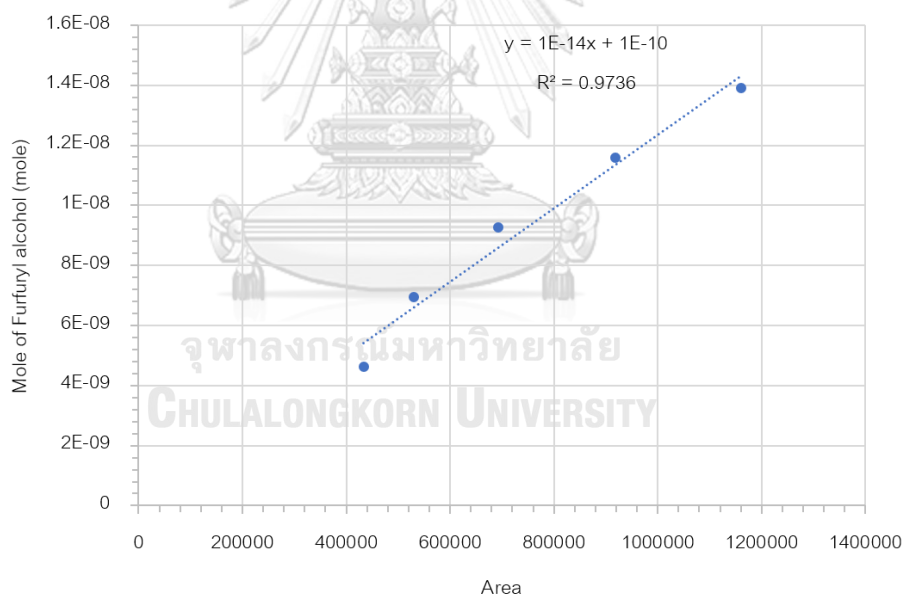


Figure E.2 The calibration curve of furfuryl alcohol

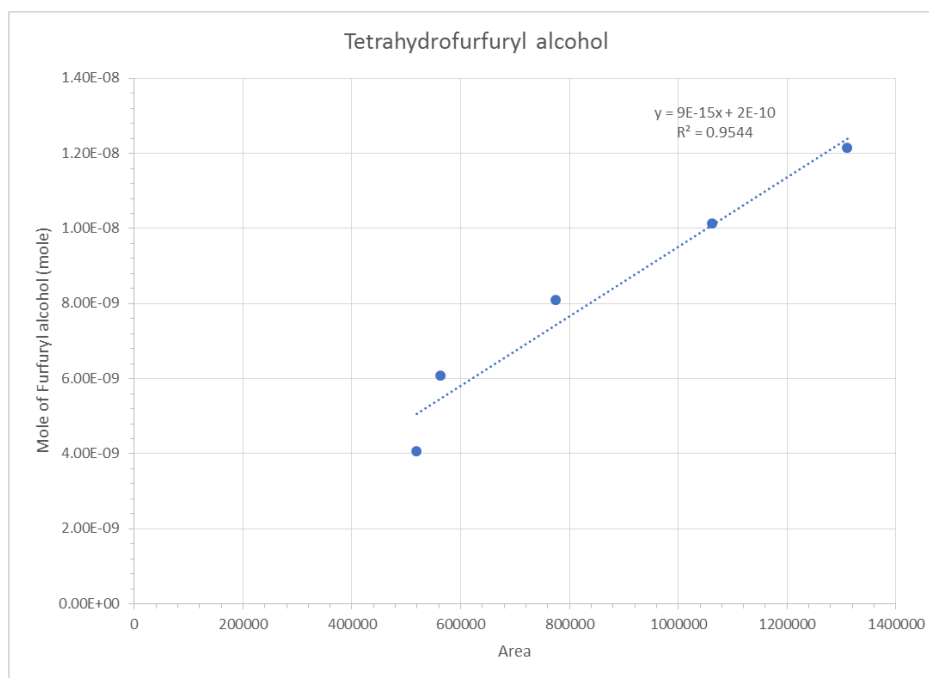


Figure E.3 The calibration curve of tetrahydrofurfuryl alcohol



VITA

NAME Kittithad Wonglekha

DATE OF BIRTH 10 February 1995

PLACE OF BIRTH Bangkok

INSTITUTIONS ATTENDED Bachelor's Degree in Chemical Engineering from Faculty of Engineering, Kasetsart University, Bangkok, Thailand in 2017 continued Master's Degree in Chemical Engineering from Faculty of Engineering, Chulalongkorn University, Bangkok, Thailand since 2017

HOME ADDRESS 25/128 Muban Chuen Kamon Niwet, Soi Nawamin 131, Nawamin Road, Nuanchan District, Bueng Kum, Bangkok, 10230